J Physiol 590.20 (2012) pp 5053–5073

The Journal of Physiology

Equal sensitivity of Cav1.2 and Cav1.3 channels to the opposing modulations of PKA and PKG in mouse chromaffin cells

Satyajit Mahapatra[1], Andrea Marcantoni[1], Annalisa Zuccotti[2], Valentina Carabelli[1] and Emilio Carbone[1]

[1]*Department of Neuroscience, NIS Center, CNISM Research Unit, 10125 Torino, Italy*
[2]*Department of Otolaryngology, University of Tübingen, 72076 Tübingen, Germany*

Key points

- Cav1.2 and Cav1.3 L-type calcium channels are highly expressed in rat and mouse chromaffin cells. Beside shaping and pacemaking action potential trains, they regulate vesicle exocytosis and endocytosis.
- L-type channels are opposingly regulated by the cAMP–PKA and cGMP–PKG pathways and their Ca^{2+} current can undergo marked up and down changes. To date, most of the reported findings on L-type channel modulation derive from the cardiac Cav1.2 isoform.
- Here, using wild-type and Cav1.3 knock out (KO) mouse chromaffin cells we show that, like Cav1.2, Cav1.3 channels are effectively modulated by PKA and PKG at basal conditions and during maximal PKA/PKG stimulation. The extent of modulation is nearly equal for both Cav1 channel isoforms.
- PKA and PKG pathways act independently on Cav1.2 and Cav1.3, producing cumulative effects that are mostly visible when activating PKA and inhibiting PKG, or *vice versa*. Under these conditions the L-type Ca^{2+} current can undergo changes of one order of magnitude.
- These extreme Cav1 channel modulations are likely to occur during different physiological conditions of the adrenal gland: 'fight-or-flight' response *vs.* relaxed states.

Abstract Mouse chromaffin cells (MCCs) express high densities of L-type Ca^{2+} channels (LTCCs), which control pacemaking activity and catecholamine secretion proportionally to their density of expression. *In vivo* phosphorylation of LTCCs by cAMP–PKA and cGMP–PKG, regulate LTCC gating in two opposing ways: the cAMP–PKA pathway potentiates while the cGMP–PKG cascade inhibits LTCCs. Despite this, no attempts have been made to answer three key questions related to the two Cav1 isoforms expressed in MCCs (Cav1.2 and Cav1.3): (i) how much are the two Cav1 channels basally modulated by PKA and PKG?, (ii) to what extent can Cav1.2 and Cav1.3 be further regulated by PKA or PKG activation?, and (iii) are the effects of both kinases cumulative when simultaneously active? Here, by comparing the size of L-type currents of wild-type (WT; Cav1.2 + Cav1.3) and $Cav1.3^{-/-}$ KO (Cav1.2) MCCs, we provide new evidence that both PKA and PKG pathways affect Cav1.2 and Cav1.3 to the same extent either under basal conditions or induced stimulation. Inhibition of PKA by H89 (5 μM) reduced the L-type current in WT and KO MCCs by ~60%, while inhibition of PKG by KT 5823 (1 μM) increased by ~40% the same current in both cell types. Given that Cav1.2 and Cav1.3 carry the same quantity of Ca^{2+} currents, this suggests equal sensitivity of Cav1.2 and Cav1.3 to the two basal modulatory pathways. Maximal stimulation of cAMP–PKA by forskolin (100 μM) and activation of cGMP–PKG by pCPT-cGMP (1 mM) uncovered a ~25% increase of L-type currents in the first case and ~65% inhibition in the

DOI: 10.1113/jphysiol.2012.236729

second case in both WT and KO MCCs, suggesting equal sensitivity of Cav1.2 and Cav1.3 during maximal PKA or PKG stimulation. The effects of PKA and PKG were cumulative and most evident when one pathway was activated and the other was inhibited. The two extreme combinations (PKA activation–PKG inhibition *vs.* PKG activation–PKA inhibition) varied the size of L-type currents by one order of magnitude (from 180% to 18% of control size). Taken together our data suggest that: (i) Cav1.2 and Cav1.3 are equally sensitive to PKA and PKG action under both basal conditions and maximal stimulation, and (ii) PKA and PKG act independently on both Cav1.2 and Cav1.3, producing cumulative effects when opposingly activated. These extreme Cav1 channel modulations may occur either during high-frequency sympathetic stimulation to sustain prolonged catecholamine release (maximal L-type current) or following activation of the NO–cGMP–PKG signalling pathway (minimal L-type current) to limit the steady release of catecholamines.

(Received 15 May 2012; accepted after revision 20 July 2012; first published online 23 July 2012)
Corresponding author E. Carbone: Department of Neuroscience, Corso Raffaello 30, 10125 Torino, Italy. Email: emilio.carbone@unito.it

Abbreviations BCC, bovine chromaffin cell; CDI, Ca^{2+}-dependent inactivation; DHP, dihydropyridine; HVA, high-voltage-activated; LTCC, L-type calcium channel; MCC, mouse chromaffin cell; PDE, phosphodiesterase; RCC, rat chromaffin cell; VDI, voltage-dependent inactivation; ω-Ctx, ω-conotoxin.

Introduction

Voltage-gated Ca^{2+} channels are highly expressed in the chromaffin cells of adrenal medulla. They trigger key Ca^{2+} signalling pathways that are vital for chromaffin cell functioning and for controlling catecholamine release during body requirement (García *et al.* 2006; Mahapatra *et al.* 2012). Among the various Ca^{2+} channel isoforms expressed in chromaffin cells, the L-type (Cav1) are particularly critical since they carry the largest proportion of Ca^{2+} currents in rodents and humans (García *et al.* 2006). Cav1 channels are directly involved in the control of action potential firing (Marcantoni *et al.* 2007, 2009, 2010), catecholamine release (García *et al.* 1984; Lopez *et al.* 1994; Kim *et al.* 1995; Nagayama *et al.* 1999; Carabelli *et al.* 2003) and vesicle retrieval (Rosa *et al.* 2007). In addition, L-type Ca^{2+} channels (LTCCs) are effectively modulated by a variety of locally released neurotransmitters or circulating hormones, which either up- or down-regulate channel gating and significantly alter the Ca^{2+} influx controlling cell functioning. These receptor-mediated modulations occur through mechanisms that are either fast and localized in membrane micro-domains (Hernández-Guijo *et al.* 1999; Hernández *et al.* 2011) or slow and remote, involving intracellular second messenger cascades, like the cGMP–PKG (Carabelli *et al.* 2002) and the cAMP–PKA pathway (Carabelli *et al.* 2001; Cesetti *et al.* 2003). The former is particularly effective in down-regulating LTCCs while the latter increases the open probability of LTCCs and the associated down-stream vesicle secretion (Carabelli *et al.* 2003). Thus, L-type Ca^{2+} currents may undergo remarkable size changes depending on the stimulus acting on chromaffin cells that could either be the consequence of the 'fight-or-flight' response, with high-frequency sympathetic discharges which elevate the level of intracellular cAMP (Anderson *et al.* 1992; Przywara *et al.* 1996), or an opposing response which increases the levels of NO and intracellular cGMP to limit Ca^{2+} flux through Cav1 channels (Schwarz *et al.* 1998; Carabelli *et al.* 2002).

The interest in LTCC modulation by hormones and neurotransmitters has further increased in the past few years since the observation that bovine, rat and mouse chromaffin cells express the two neuronal Cav1 channel isoforms, Cav1.2 and Cav1.3 (García-Palomero *et al.* 2001; Baldelli *et al.* 2004; Marcantoni *et al.* 2010; Peréz-Alvarez *et al.* 2011). As for the neuronal isoforms, the Cav1.2 and Cav1.3 of mouse chromaffin cells possess strong sensitivity to dihydropyridine (DHP) agonists and antagonists but exhibit rather different functional properties that derive from their distinct voltage range of activation and time course of voltage- (VDI) and Ca^{2+}-dependent inactivation (CDI) (Koschak *et al.* 2001; Xu & Lipscombe, 2001). Cav1.3 activates at 10–20 mV more negative voltages than Cav1.2 (Mangoni *et al.* 2003; Lipscombe *et al.* 2004; Mahapatra *et al.* 2011) and has faster activation but slower and less complete VDI as compared with Cav1.2 (Koschak *et al.* 2001; Xu & Lipscombe, 2001). In addition, in MCCs Cav1.3 is more tightly coupled to fast-inactivating BK channels than Cav1.2 (Marcantoni *et al.* 2010; Vandael *et al.* 2010) and is able to drive SK channels near resting potentials (Vandael *et al.* 2011). All these properties explain the unique role that Cav1.3 plays in setting the pacemaking current driving action potential (AP) firings during spontaneous cell activity or regulating burst firing during prolonged depolarization. In fact, despite Cav1.2 and Cav1.3 carrying

equal amounts of Ca^{2+} currents, loss of Cav1.3 channels in MCCs causes: (i) a reduction of the Ca^{2+} currents that drive AP firing in MCCs, (ii) a reduced percentage of spontaneously firing cells in physiological KCl solutions and (iii) anomalous AP bursts and prolonged plateau depolarizations in response to DHP agonists (Marcantoni *et al.* 2010; Vandael *et al.* 2010; Mahapatra *et al.* 2011). At variance with this, Cav1.2 contributes mostly to the Ca^{2+} influx during the AP upstroke and thus appears more critical in controlling Ca^{2+} signalling during fast repeated depolarization.

Given these basic functional differences and the limited information presently available on PKA- and PKG-mediated modulation of Cav1.3 channels (Marshall *et al.* 2011; see Catteral, 2011 for a review), we thought it would be of interest to assay how Cav1.2 and Cav1.3 are effectively modulated by the two opposing pathways which may drive significant changes to the size of L-type currents and Ca^{2+} signalling regulating chromaffin cells activity. Here, using the Cav1.3$^{-/-}$ KO mouse (Platzer *et al.* 2000), we compared the potentiating effect of cAMP–PKA and the inhibitory action of cGMP–PKG on the L-type currents of WT and Cav1.3$^{-/-}$ KO MCCs and show that Cav1.2 and Cav1.3 are equally sensitive to the two modulatory pathways. This occurs at basal conditions, where both kinases are already active, and during PKA- or PKG-induced stimulation. The two modulatory pathways act independently on both channel isoforms, so that extreme conditions (activation of PKA and inhibition of PKG or *vice versa*) induce cumulative effects leading to Ca^{2+} current amplitudes that can vary by one order of magnitude (from 18 to 180% of control size). This L-type current 'plasticity' may occur under elevated sympathetic stimulation during cAMP-mediated sustained release of catecholamines in response to stressful conditions (Przywara *et al.* 1996; Wakade, 1998) or during activation of the NO–cGMP–PKG pathway to rapidly limit catecholamine release (Oset-Gasque *et al.* 1994; Rodríguez-Pascual *et al.* 1996).

Methods

Ethical approval

Ethical approval was obtained for all experimental protocols from the University of Torino Animal Care and Use Committee, Torino, Italy. All experiments were conducted in accordance with the National Guide for the Care and Use of Laboratory Animals adopted by the Italian Ministry of Health. Every effort was made to minimize animal suffering and the number of animals used. For removal of tissues, animals were deeply anaesthetized with CO_2 inhalation and rapidly killed by cervical dislocation.

Isolation and culture of WT and Cav1.3$^{-/-}$ mouse chromaffin cells

Chromaffin cells were obtained from young (1–3 months old) male C57BL/6N mice. As for our previous work (Marcantoni *et al.* 2010; Mahapatra *et al.* 2011), Cav1.3$^{-/-}$ mice (Platzer *et al.* 2000) were obtained from the animal house of the Eberhard Karls Universität Tübingen (Germany), which breeds animals under SPF conditions and provided us with the respective health certificates that are on file. Chromaffin cells were isolated and cultured following a slightly modified procedure of the method described elsewhere (Marcantoni *et al.* 2009). After removal, adrenal glands were placed in Ca^{2+}- and Mg^{2+}-free Locke solution (in mM: 154 NaCl, 5.6 KCl, 3.6 $NaHCO_3$, 5.6 glucose, 10 Hepes (pH 7.2) and 1% penicillin–streptomycin (pen-strep) solution), and cleaned free from fat and outer cortical layer tissues. The medullas were incubated in digestion solution (mentioned below) for 30 min at 37°C with slight regular-interval shaking, followed by removal of digestion solution and rinsing twice with washing solution (see below). The medullas were then carefully placed in 1 ml of enriched DMEM solution (DMEM + 1% pen-strep + 15% fetal bovine serum (FBS)) and gently triturated with a 200 μl pipette tip to dissociate the cells. Aliquots of 100 μl of the concentrated cell suspension were then placed in four-well plastic dishes, pre-treated with poly-L-ornithine (0.5 mg ml^{-1}) and laminin (10 μg ml^{-1} in L-15 carbonate). The cells were allowed to settle before supplementing with 1.9 ml of enriched DMEM solution. The plates were incubated at 37°C with 5% CO_2 and used after 1 day of incubation. Digestion solution (20–25 U ml^{-1} of papain (Worthington Biochemical, Lakewood, NJ, USA) plus 20 μl of 0.2 mg ml^{-1} DNase (Sigma)) was solubilised in 1 ml of DMEM solution (Gibco, Invitrogen) containing 1.5 mM L-cysteine, 1 M $CaCl_2$ and 0.5 mM EDTA. Washing solution was DMEM with 1 mM $CaCl_2$ and 10 mg ml^{-1} bovine serum albumin (Sigma, USA). FBS (Sigma, USA) used in enriched DMEM media was heat inactivated at 56°C for 30 min prior to use.

Voltage-clamp recordings

Voltage-clamp recordings were made in the perforated-patch configuration using either an EPC-9 amplifier with corresponding software Pulse (HEKA, Elektronik, Lambrecht, Germany) or an Axopatch 200-A amplifier with pCLAMP 10.2 software (Molecular Devices Inc., Sunnyvale, CA, USA). Patch pipettes were made of thin borosilicate 1.5–1.8 mm glass tube capillaries (Kimble Glass Inc., NJ, USA), fire-polished and those with a series resistance of 2–3 MΩ were used for the experiment. Series resistance was adjusted automatically.

Ca^{2+} currents were evoked by a step depolarization to +10 mV from a V_h of either −80 or −50 mV for 20 ms and repeated at regular intervals (10–20 s). The patch pipette solution contained (in mM): 135 Cs-$MeSO_3$, 8 NaCl, 2 $MgCl_2$ and 20 Hepes, pH 7.4 with CsOH) supplemented with amphotericin B (Sigma), used at a final concentration of 500 μg ml^{-1}. The external bath solution contained (in mM): 130 NaCl, 5 TEA-Cl, 2 $CaCl_2$, 2 $MgCl_2$, 10 Hepes and 10 glucose, pH 7.4 adjusted with NaOH, supplemented with freshly added tetrodotoxin (TTX, 300 nM final concentration) before use.

The procedure to achieve optimal perforated-patch recording conditions with amphotericin B dissolved in dimethyl sulfoxide (DMSO) was similar to that described previously (Cesetti *et al.* 2003; Marcantoni *et al.* 2009). Current traces were acquired at 10 kHz and filtered using a low-pass Bessel filter set at 1–2 kHz. Fast capacitative transients during step depolarization were minimized on-line by patch-clamp analog compensation. Uncompensated capacitative currents were further reduced by subtracting the averaged currents in response to P/4 hyperpolarizing pulses (Marcantoni *et al.* 2010). Liquid junction potential was not corrected since ionic content of the pipette and the bath solutions were unchanged in most experiments. All the experiments were performed at room temperature (22–25°C).

Statistical analyses were performed using SPSS statistics 20 software (IBM, USA) and all the graphs were made using Microcal Origin Pro (version 6; Northampton, MA, USA). Drug effects were calculated as (100 × {(control – drug)/(control)}) and the normalized percentage of Ca^{2+} current changes are given as mean ± standard error of the mean (SEM) for a number of cells (n). Student's t test was used to evaluate significant differences of drug effect *vs.* control on the same cell or between WT and KO cells. One-way ANOVA followed by a Bonferroni *post hoc* test was used to determine differences on the effects of several compounds tested separately on the same cell. Statistical significance (P) was set at $P < 0.05$ using 2-tailed Student's t test and one-way ANOVA. The corresponding P values are indicated as: $^{*}0.05 > P \geq 0.01$; $^{**}0.01 > P \geq 0.001$; $^{***}P < 0.001$.

Solutions

Nifedipine, H89, forskolin, 8-pCPT-cGMP (cGMP) and KT 5823 were purchased from Sigma; tetrodotoxin citrate (TTX) was purchased from Tocris Bioscience (Bristol, UK). ω-Conotoxin-MVIIC (ω-Ctx-MVIIC), ω-conotoxin-GVIA (ω-Ctx-GVIA) and SNX 482 were purchased from Peptide Institute (Osaka, Japan) and were used for blocking P/Q-, N- and R-type calcium channels as previously described (Marcantoni *et al.* 2010). Nifedipine was used at a final concentration of 3 μM from a 1 mM stock solution dissolved in 98% ethanol, and stored in the dark at 4°C (Magnelli *et al.* 1995). Stock solutions of forskolin (10 mM) and H89 (1 mM) were made in 20% DMSO, and were used at final concentrations of 1–100 μM (forskolin) and 1–5 μM (H89). ω-Ctx-MVIIC, ω-Ctx-GVIA and SNX 482 were dissolved in distilled water and kept in stock aliquots (100 μM, 160 μM and 20 μM, respectively) at −20°C until their use at the final concentration required. At their final concentrations, the drugs were acutely perfused on the cell at a rate of ∼0.15 ml min^{-1} using a multi-barrelled perfusion system with five inlets and a common outlet (Carabelli *et al.* 1998).

RNA extraction, reverse transcription and PCR amplification

For RNA isolation, mouse adrenal medulla were dissected with small forceps, immediately frozen in liquid nitrogen, and stored at −80°C before use. RNA was isolated using the RNeasy mini kit (QIAGEN, Hilden, Germany) following the manufacturer's instructions. After reverse transcription using a Sensiscript RT kit (QIAGEN), PCR was performed with PuReTaq Ready-To-Go PCR beads (GE Healthcare, Munich, Germany) using specific primers: PKA Iα (Prkar1a NM_021880) forward: 5′-CTGTGGGGCATCGACCGAGA-3′, reverse: 5′-TGTCTGAGCACGGGCCAAGG-3′; PKA Iβ (Prkar1b NM_008923) forward: 5′-ATCTACGGCACCCCCAG AGC-3′, reverse: 5′-ACACACTTGAGGGGACCCCG-3′; PKA IIα (Prkar2a NM_008924) forward: 5′-AGTGAC TCGGACTCGGAAGATG-3′, reverse: 5′-CTGCCAC GGTTGTCATACTGA-3′; PKA IIβ (Prkar2b NM_011158) forward: 5′-TAAACCGGTTCACAAGGCGTG-3′, reverse: 5′-CCTTGGTCAATTACGTGTTCCC-3′; PKA catalytic α (Prkaca NM_008854) forward: 5′-CCAAGAAGGG CAGCGAGCAG-3′, reverse: 5′-TGGGATGGGAAC CGCACCTT-3′; PKA catalytic β (Prakab NM_011100) forward: 5′-GCCCCACGCCCGTTTCTATG-3′, reverse: 5′-CGCCGTTCTTCAGGTTCCCG-3′; cGK Iα (Prkg1 NM_001013833) forward: 5′-CGCCAGGCGTTCCGGA AGT-3′, reverse: 5′-GTGCAGAGCTTCACGCCTT-3′; cGK Iβ (Prkg1 NM_011160) forward: 5′-CTCCGCGGA AGCCCACCGCCTT-3′, reverse: 5′-TCAAACTTCCCAT CTTCCATG-3′; cGK II (Prkg1 ENSMUST00000031277) forward: 5′-TCAGGAACGGGAGTACCACCT-3′, reverse: 5′-TCAGGGCATCTGTGATGAGCT-3′.

Results

MCCs express four PKA regulatory subunits and three PKG isoforms

To validate PKA and PKG as potential proteins responsible for LTCCs phosphorylation in MCCs, in a first series of experiments we analysed the expression of different PKA

regulatory (I-α, I-β, II-α and II-β) and catalytic subunits (C-α and C-β) and PKG isoforms (I-α, I-β and II). Their expression was verified by RT-PCR at transcriptional level in the medulla of adrenal glands isolated from six mice (1–3 months old) using specific primers (see Methods). The amplification products of PKA I-α, I-β, II-α, II-β, C-α, C-β and PKG I-α, I-β and II with the appropriate size were found in murine adrenal medulla (M) as well as in brain (B), which was used as positive control (Fig. 1). Given the existence of PKA and PKG isoforms in MCCs, we next tested the effect of the two kinases on both Cav1.2 and Cav1.3 either under basal activity or under maximal stimulation.

Cav1 are the only voltage-gated Ca^{2+} channels basally potentiated by PKA in MCCs

MCCs express LTCCs (Cav1) and non-LTCCs (Cav2) and exhibit *I–V* characteristics that peak at about +10 mV in 2 mM external Ca^{2+} (Marcantoni *et al.* 2009, 2010). LTCCs contribute to nearly 50% of the total Ca^{2+} current activated by brief step depolarization to +10 mV. The current is carried by an almost equal ratio of Cav1.2 and Cav1.3 channels expressed in MCCs (Marcantoni *et al.* 2010). MCCs also possess basal levels of cAMP (Marcantoni *et al.* 2009) which could regulate a PKA-mediated phosphorylation of Cav1.2 and Cav1.3 and contribute to basally potentiated L-type Ca^{2+} currents (Cesetti *et al.* 2003). Basal levels of PKA, however, could as well down-regulate Cav2 channels (Surmeier *et al.* 1995; Momiyama & Fukazawa, 2007), partially compensating the enhancing effects on LTCCs. To quantify the percentage of PKA-mediated phosphorylation of Ca^{2+} channels under basal conditions, we tested the effect of the specific PKA antagonist H89 on Ca^{2+} current amplitudes in the presence or absence of selective Ca^{2+} channel blockers to separate a possible up-regulation of LTCCs from a down-regulation of non-LTCCs. Ca^{2+} currents were evoked by brief (20 ms) depolarizing pulses to +10 mV from a holding potential of −80 or −50 mV, repeated every 15 s in 2 mM external Ca^{2+}. The brief step depolarization was preferred to limit Ca^{2+} influx and slow down the physiological Ca^{2+} channel run-down.

As shown in Fig. 2, application of 5 μM H89 caused a marked down-regulation of Ca^{2+} currents (25.7 ± 1.9%, $n = 9$) which was prevented when the PKA inhibitor was applied simultaneously with nifedipine (3 μM) (Fig. 2*A–C*). The mean reduction of peak currents in the presence of nifedipine alone was 36.5 ± 0.9% and not significantly different when H89 was added (37.6 ± 1.0%, $n = 9$; $P = 1.0$) (Fig. 2*D*). In four of these cells, H89 caused an apparent slight increase of the current that was, however, not statistically significant and that could be due to the removal of a PKA-mediated basal inhibition of non-L-type Cav2 channels (see below). The block by nifedipine required few seconds to reach maximal effects while inhibition by H89 was significantly slower, mostly due to its remote action on PKA and Cav1 channels. The onset and offset of H89 action required 90–120 s to reach steady-state conditions and had no major effects on the time constant of channel activation. The mean half-time to peak ($t_{1/2}$) was 1.13 ± 0.07 ms without and 1.05 ± 0.05 ms with H89. In a few MCCs,

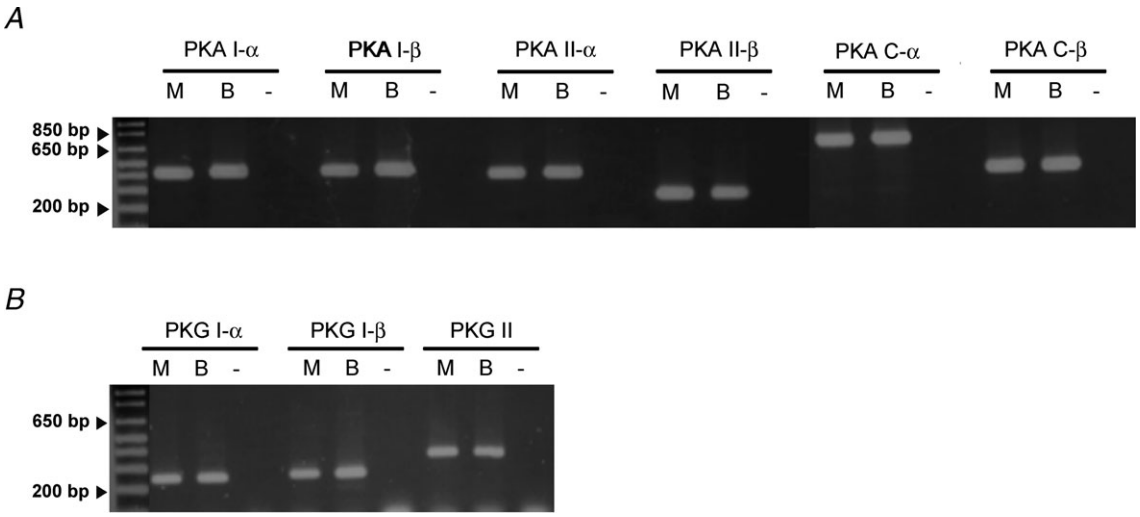

Figure 1. RT-PCR analyses of PKA and PKG subunits expressed in mouse chromaffin cells
Expression analysis at the transcription level of PKA regulatory (I-α, I-β, II-α, II-β) and catalytic subunits (C-α, C-β) (upper panel) and PKG I-α, I-β, II (lower panel) by RT-PCR in adrenal medulla (M) cDNA. Adult whole brain (B) cDNA was used as positive control. In the negative control (−), no cDNA was added. $n = 6$ animals, each experiment was done in triplicate. All experimental details and primers are given in the Methods.

we also tested the effects of 1 μM H89 (Carabelli *et al.* 2001) and found only a significantly prolonged time to reach steady-state values with no changes in the percentage of inhibition. Thus, to shorten the duration of the experiments and to limit the Ca^{2+} current run-down, we chose to use H89 at 5 μM, being aware that several kinases (S6K1, MSK1 and ROCK-II), besides PKA, could be inhibited by these concentrations (Davies *et al.* 2000). These kinases, however, are not expected to contribute significantly to basal Cav1 channels phosphorylation (see Discussion).

We also found that the H89-induced inhibition was similar at different membrane potentials, as shown by the proportional depression of the *I–V* characteristics induced by H89 at all potentials (Fig. 2*E*). These preliminary findings indicate that of the Ca^{2+} channels expressed in MCCs, LTCCs are those preferentially up-regulated by cAMP–PKA under basal conditions. Inhibition of the resting PKA-mediated phosphorylation of LTCCs causes a marked reduction of total Ca^{2+} currents, which is independent of membrane potential. This justifies the choice of testing the effects of PKA inhibitors or activators at +10 mV where Ca^{2+} currents reach maximal amplitude in 2 mM Ca^{2+} and the fastest asymptotic values of activation kinetics (Marcantoni *et al.* 2010).

A selective inhibition of LTCCs by H89 is further confirmed by the results of Fig. 3 in which H89 is shown to preserve its depressive action on LTCCs after having blocked Cav2 channels with the following toxin mixture: ω-conotoxin (ω-Ctx) MVIIC (10 μM), ω-Ctx-GVIA (3.2 μM) and SNX 482 (SNX; 0.4 μM), which is able to fully block the Ca^{2+} current remaining after nifedipine (3 μM) application at $V_h = -50$ mV (Marcantoni *et al.* 2010). The three toxins caused a marked reduction of I_{Ca} (54.8 ± 1.9%) but preserved the inhibitory effects of H89 (29.4 ± 2.8%, $^{***}P < 0.001$; $n = 7$) (Fig. 3*A–C*). Although not statistically significant, the inhibition of I_{Ca} was slightly larger than the 25.7% reduction observed in the absence of Cav2 channel blockers (Fig. 2*D*). This could be due to the existence of an effective basal PKA-mediated up-regulation of LTCCs (~30% of the total current) and a possibly 3–4% opposite action on Cav2 channels, not clearly resolved here but supported by the data described in the following section.

Cav 1.2 and Cav 1.3 are equally sensitive to basal PKA inhibition by H89

Given that LTCCs are the only Ca^{2+} channels basally up-regulated by PKA, we next tested how individually Cav1.2 and Cav1.3 contributed to the up-regulation of LTCCs by comparing the effects of H89 in WT and Cav1.3$^{-/-}$ KO MCCs. WT MCCs express both Cav1.2 and Cav1.3, while KO MCCs express only Cav1.2 channels. In addition, we have already shown that Cav1.2 and Cav1.3 contribute almost equally to the total L-type current in MCCs (Marcantoni *et al.* 2010; Mahapatra *et al.* 2011). Thus, by quantifying the L-type currents in WT

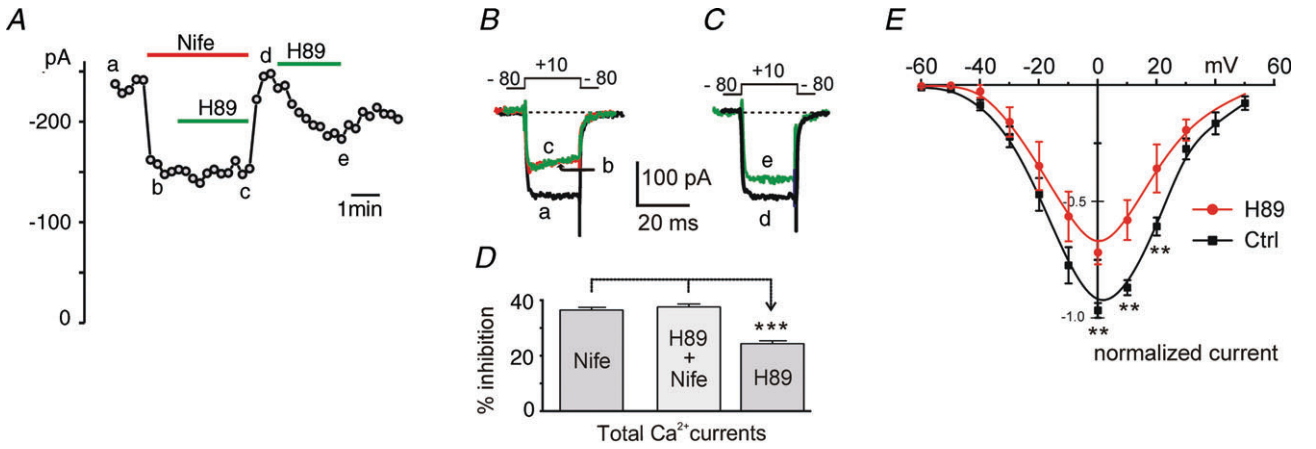

Figure 2. The PKA blocker H89 reduces the basally potentiated I_{Ca}, in the absence but not in the presence of LTCC block by nifedipine in WT MCCs
A, plot of peak current amplitudes recorded as a function of time in 2 mM Ca^{2+}. The inhibitory effect of H89 (5 μM) was hindered in the presence of nifedipine (3 μM). Step depolarizations of 20 ms to +10 mV were evoked from −80 mV (V_h) and repeated every 15 s. *B* and *C*, current traces recorded at the time indicated by the letters in *A*. *D*, mean percentage inhibition of I_{Ca} by H89 in presence and absence of LTCCs block by nifedipine and H89 alone are shown ($n = 9$). The two mean values with nifedipine alone and in the presence of H89 are not statistically different ($P = 1.0$), whereas inhibition of I_{Ca} by H89 alone *vs.* nife and H89 + nife was found to be significantly different ($^{***}P < 0.001$, using one-way ANOVA followed by Bonferroni *post hoc* test). *E*, *I–V* relationships of total Ca^{2+} currents in control ($n = 9$) and during application of 5 μM H89 ($n = 5$) obtained by brief depolarizations (20 ms) to the indicated voltages ($^{**}P < 0.01$ *vs.* control using unpaired Student's *t* test). Holding potential −80 mV.

and KO MCCs and the effects of H89, we thought we could estimate the effective basal up-regulation of the two LTCCs. The results are shown in Fig. 4. Each MCC was first tested for the blocking potency of nifedipine and then for the inhibitory action of H89 (Fig. 4*A* and *B*). In WT MCCs nifedipine blocked on average $39.3 \pm 4.1\%$ ($n = 8$) of the currents and H89 caused a depression of $27.7 \pm 3.4\%$. In Cav1.3$^{-/-}$ KO MCCs expressing only Cav1.2 channels, the block by nifedipine was reduced to nearly half ($21.6 \pm 1.7\%$, $^{**}P = 0.003$; $n = 8$) from WT and the same occurred for the H89 depression ($12.8 \pm 2.3\%$, $^{**}P = 0.003$) of the total current. Normalizing the percentage of H89 inhibition to the size of L-type currents, it was evident that H89 inhibited with the same potency both WT (70%) and KO MCCs (60%) ($P = 0.18$; Fig. 4*E*), suggesting that both Cav1 isoforms were equally up-regulated at rest by the active cAMP–PKA pathway. Notice that at $V_h = -80$ mV full block of Cav1.3 by 3 μM nifedipine is partially underestimated by 10–15% (Xu & Lipscombe, 2001; Mahapatra *et al.* 2011) in WT MCCs. However, even considering the percentage of unblocked Cav1.3 current, both LTCC isoforms (Cav1.2 and Cav1.3) show equal sensitivity to PKA under basal conditions.

PKA activation equally potentiates Cav 1.2 and Cav 1.3

The potent inhibition (~65%) of LTCCs by H89 suggests that LTCCs are markedly phosphorylated at their PKA sites under basal conditions in MCCs. Assuming that PKA phosphorylation sites of LTCCs are still not basally saturated, we next tested whether PKA activation could further potentiate Cav1.2 and Cav1.3 to determine the maximal current that these two channels could potentially carry when fully phosphorylated by PKA. A straightforward way to test this was to increase intracellular cAMP levels by activating adenylyl cyclase (AC) by forskolin and comparing the I_{Ca} potentiation in WT and Cav1.3$^{-/-}$ KO MCCs.

To our surprise, however, when tested on the total Ca^{2+} currents, 1–100 μM forskolin caused either no effects or minor inhibitions ($12.8 \pm 0.9\%$ current reduction, $n = 11$). We never observed significant potentiating effects (Fig. 5*A* and *B*). On the contrary, there were always large inhibitions in the presence of nifedipine ($21.8 \pm 2.5\%$, $n = 5$; $^{*}P = 0.02$) (Fig. 5*C–E*), that suggested a hindered potentiating effect of forskolin on LTCCs. Thus, we concluded that forskolin had opposing actions on LTCCs and non-LTCCs: an up-regulatory effect on Cav1 channels that was completely masked by a more robust inhibition of N-, P/Q- and R-type channels. This latter action resembled the D_1 receptor-mediated inhibition of N- and P/Q-channels in neostriatal (Surmeier *et al.* 1995) and basal forebrain neurones (Momiyama & Fukazawa, 2007). Thus, given the existence of these two opposing actions, we decided to test the effects of forskolin (100 μM) on LTCCs after having blocked the non-LTCCs with the toxin mixture previously used (Fig. 3*A*).

As shown in Fig. 6*A* and *B*, the half block of Cav2 channels by the toxins (ω-Ctx-MVIIC + ω-Ctx-GVIA + SNX 482) was fast and complete within 60 s. After Cav2 channel block, the remaining LTCC currents in WT (Cav1.2 + Cav1.3) and KO MCCs (Cav1.2) were around 50% and 25% ($51.7 \pm 2.6\%$, $n = 9$ and $27.3 \pm 1.8\%$, $n = 8$,

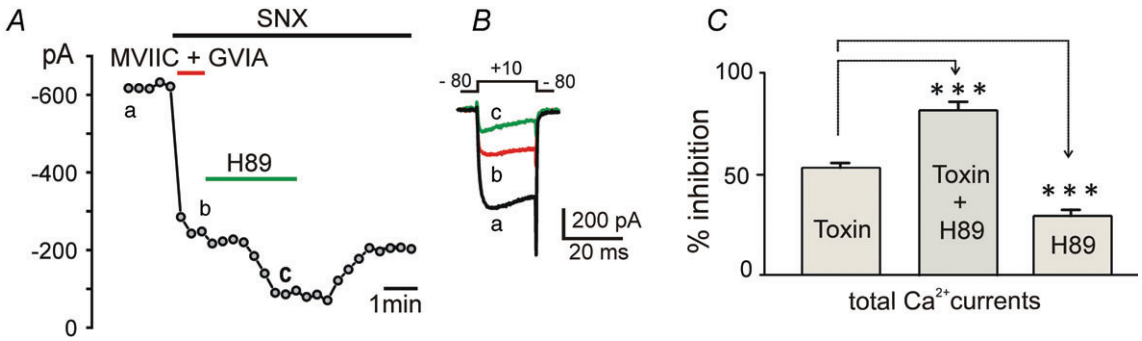

Figure 3. Block of N-, P/Q- and R-types of HVA channels does not prevent the inhibitory effect of H89 in WT MCCs

A, the reversible inhibitory effect of H89 (5 μM) was always visible following the block of Cav2 channels by ω-Ctx-MVIIC (10 μM) + ω-Ctx-GVIA (3.2 μM) + SNX 482 (0.4 μM) ($n = 7$). Peak Ca^{2+} currents were recorded as a function of time in 2 mM extracellular Ca^{2+}. SNX 482 was present in all the solutions, including wash. Step depolarization of 20 ms to +10 mV were evoked from −80 mV (V_h) and repeated every 20 s. *B*, current traces recorded at the time indicated by the letters in *A*. *C*, mean percentage inhibition of I_{Ca} calculated from $n = 7$ cells shows that I_{Ca} block by the toxin mixture alone and with H89 are statistically significant ($^{***}P < 0.001$, using one-way ANOVA with Bonferroni *post hoc* test). The calculated I_{Ca} inhibition by H89 ($29.4 \pm 2.8\%$) ((toxin + H89) – toxin) is also significantly different from the toxin block ($^{***}P < 0.001$).

$^{***}P < 0.001$; Fig. 6*C*), indicating equal contribution of Cav1.2 and Cav1.3 channels to the toxin-resistant current. Application of forskolin (100 μM) together with SNX led to a net potentiation of LTCCs, which was slow at the beginning, as expected for forskolin to diffuse inside the cell and activate the adenylyl cyclase. Maximal potentiation of LTTCs was achieved within 60–90 s. In WT and in KO MCCs, the I_{Ca} increase by forskolin was $13.4 \pm 0.9\%$ ($n = 9$) and $7.2 \pm 1.1\%$ ($^{**}P = 0.006$; $n = 8$), respectively (Fig. 6*D*). Normalization of these values to the L-type current size shows that full phosphorylation of Cav1.2 and Cav1.3 causes a ~25% increase of L-type currents (Fig. 6*E*), with no prevalence of one isoform over the other ($P = 0.92$). This confirms that Cav1.2 and Cav1.3 are equally liable to PKA potentiation, irrespectively of whether the V_h was maintained rather negative (−80 mV) or near the resting potential (−50 mV).

As a final control we also tested if the forskolin-induced potentiation of LTCCs was prevented by H89. Figure 6*F* and *G* shows that this is indeed the case. After blocking the Cav2 channels by the toxin mixture, the reversible potentiation of $I_{Ca\text{-}L}$ by forskolin was around 25% ($24.0 \pm 1.5\%$). However, in the presence of L-type channel inhibition by H89 ($40.8 \pm 2.4\%$), when forskolin (100 μM) was applied, it did not produce any further changes ($40.0 \pm 2.5\%$; $P = 0.82$). This supports the conclusion that Cav1.2 and Cav1.3 of MCCs are equally sensitive to the cAMP–PKA elevation induced by forskolin and H89 fully prevents it.

cGMP selectively inhibits LTCCs

Activation of PKG is shown to inhibit neuronal LTCCs (Sumii & Sperelakis, 1995; Carabelli *et al.* 2002; Yang *et al.* 2007), but whether this action is specific for LTCCs or could affect Cav2 channels as well has not been proved yet. To assess this issue, we first tested the inhibitory effects of the membrane-permeable cGMP analogue 8-pCPT-cGMP (0.1–1 mM) on total I_{Ca} in the

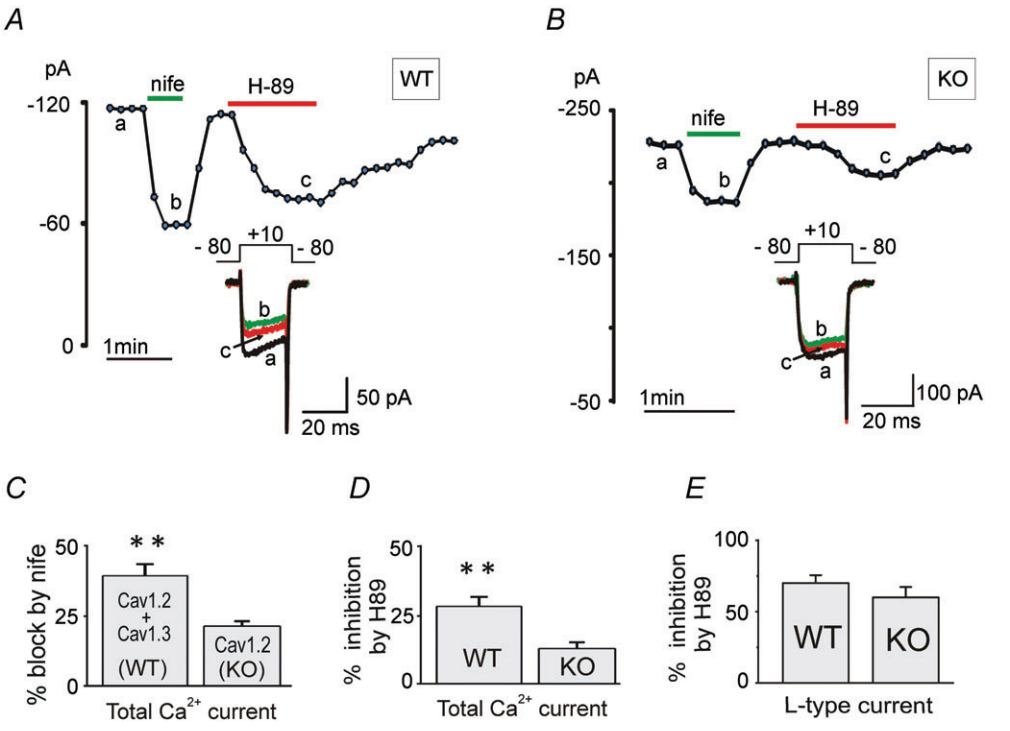

Figure 4. Comparative inhibition of I_{Ca} by nifedipine and H89 in WT and Cav1.3$^{-/-}$ KO MCCs
A, Ca^{2+} current amplitude *vs.* time plot showing a typical inhibition of I_{Ca} in WT MCCs by nifedipine (3 μM) and H89 (5 μM). Inset shows the current traces recorded at the time indicated by the letters. Currents were evoked using a depolarizing pulse of 20 ms to +10 mV from −80 mV (V_h) repeated every 10 s in 2 mM extracellular Ca^{2+}. *B*, I_{Ca} inhibition induced by nifedipine and H89 in Cav1.3$^{-/-}$ KO MCCs; same recording conditions as in *A*. *C*, mean I_{Ca} inhibition induced by nife in WT and KO MCCs, which represent the size of LTCC currents in WT (Cav1.2 + Cav1.3) and KO MCCs (Cav1.2) MCCs. They are statistically different ($^{**}P = 0.003$, using unpaired Student's *t* test). *D*, inhibition of basally PKA-potentiated I_{Ca} by H89 in WT and in KO MCCs ($^{**}P = 0.003$). *E*, percentage inhibition of LTCC currents by H89 in WT and in KO MCCs are not statistically different ($P = 0.18$).

absence and presence of nifedipine. As shown in Fig. 7, 8-pCPT-cGMP (1 mM) produced a marked inhibition of total Ca^{2+} currents at +10 mV (36.5 ± 2.2%, $n = 4$, Fig. 7*A*) that was independent of membrane voltage as shown by the nearly identical percentage of current block from −50 to +50 mV (Fig. 7*B*). Inhibition required nearly 80–120 s to reach maximal values, was fully reversible and rather similar if using 0.1 or 1 mM 8-pCPT-cGMP (see below). Complete washing required around 2 min. The inhibitory action of 8-pCPT-cGMP was fully prevented when LTCCs were blocked by 3 μM nifedipine and Ca^{2+} currents were carried only by Cav2 channels (Fig. 7*C*). Block by nifedipine was maximal within 60 s (35.2 ± 3.3%) and did not further increase when 8-pCPT-cGMP was applied for 120–180 s (36.7 ± 1.7%, $n = 4$; $P = 1$) (Fig. 7*D*). To confirm that cGMP selectively acts on LTCCs, we also tested 8-pCPT-cGMP before and after blocking Cav2 channels with the toxin mixture (ω-Ctx-MVIIC + ω-Ctx-GVIA + SNX 482) (Fig. 8). Except for the first part of cGMP effect alone and the last part of the wash, SNX was present in all solutions, including the first wash. Mean percentage of inhibition

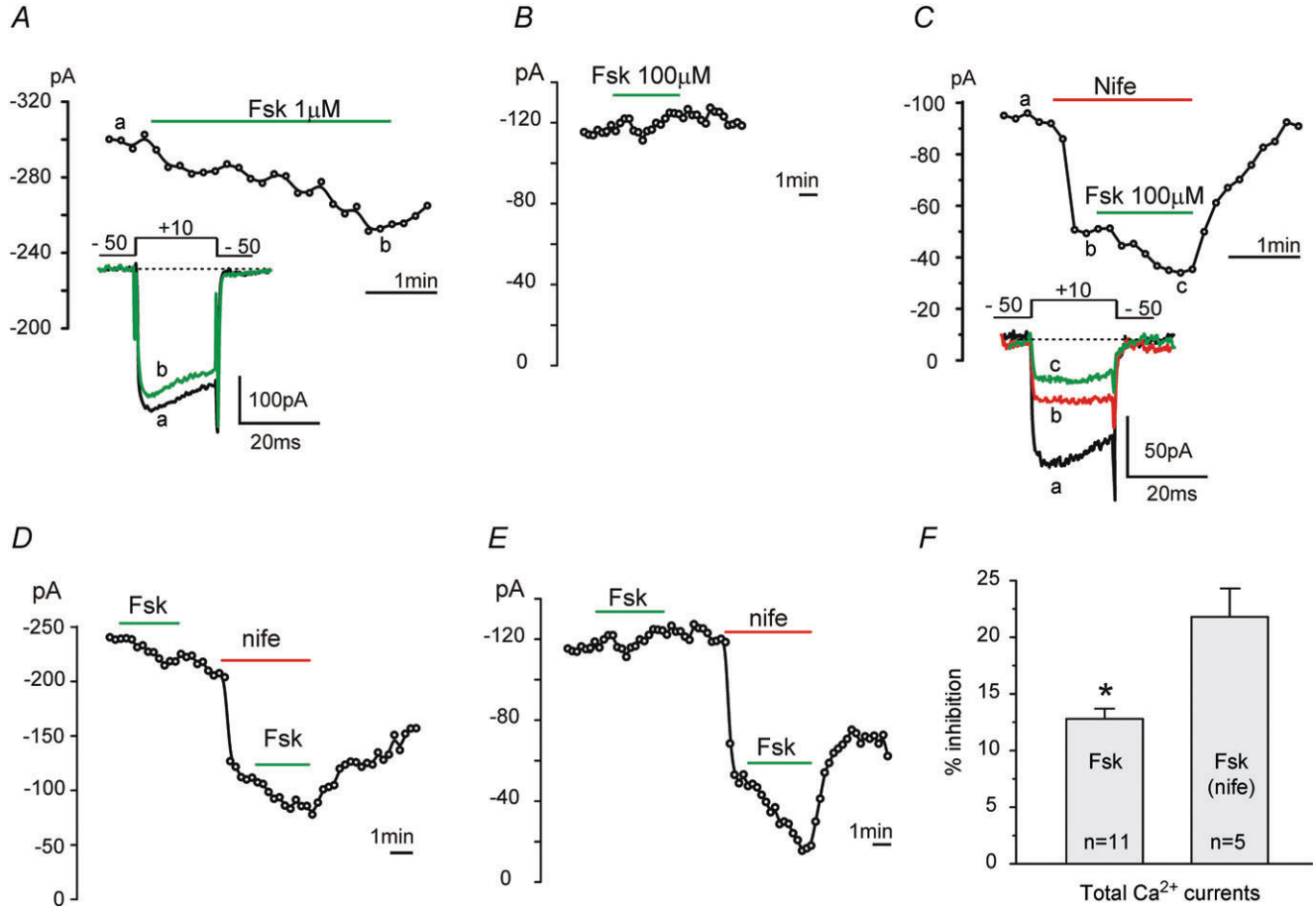

Figure 5. Forskolin has a moderate inhibitory effect on I_{Ca} in WT MCCs which turns to a marked inhibition in the presence of LTCC block by nifedipine
A, example of Ca^{2+} current inhibition induced by the adenylyl cyclase activator forskolin (Fsk) observed in 90% of MCCs. I_{Ca} was evoked by a 20 ms pulse to +10 mV from −50 mV repeated every 10 s. The bath solution contained 2 mM Ca^{2+}. Exposure to forskolin (1 μM) caused maximal inhibition within 120–150 s. *B*, example of a mixed inhibition and potentiation of I_{Ca} by forskolin (100 μM) observed in the remaining 10% of MCCs. *C*, in the presence of nifedipine (3 μM), application of forskolin (100 μM) produced only marked inhibitions of I_{Ca}. Maximal effects were observed within 60 s of forskolin exposure. *D* and *E*, in these two representative cells, application of forskolin caused either inhibition or a mixed response of potentiation and inhibition on I_{Ca}. After LTCC block by nifedipine (3 μM), forskolin caused inhibitions greater than those observed before DHP application. Same protocol as in *A* and *C*, except that the pulse was repeated every 15 s. *F*, percentage inhibitions of I_{Ca} by 100 μM forskolin before and after nifedipine block of LTCCs. They are significantly different (*$P = 0.02$, using unpaired Student's *t* test).

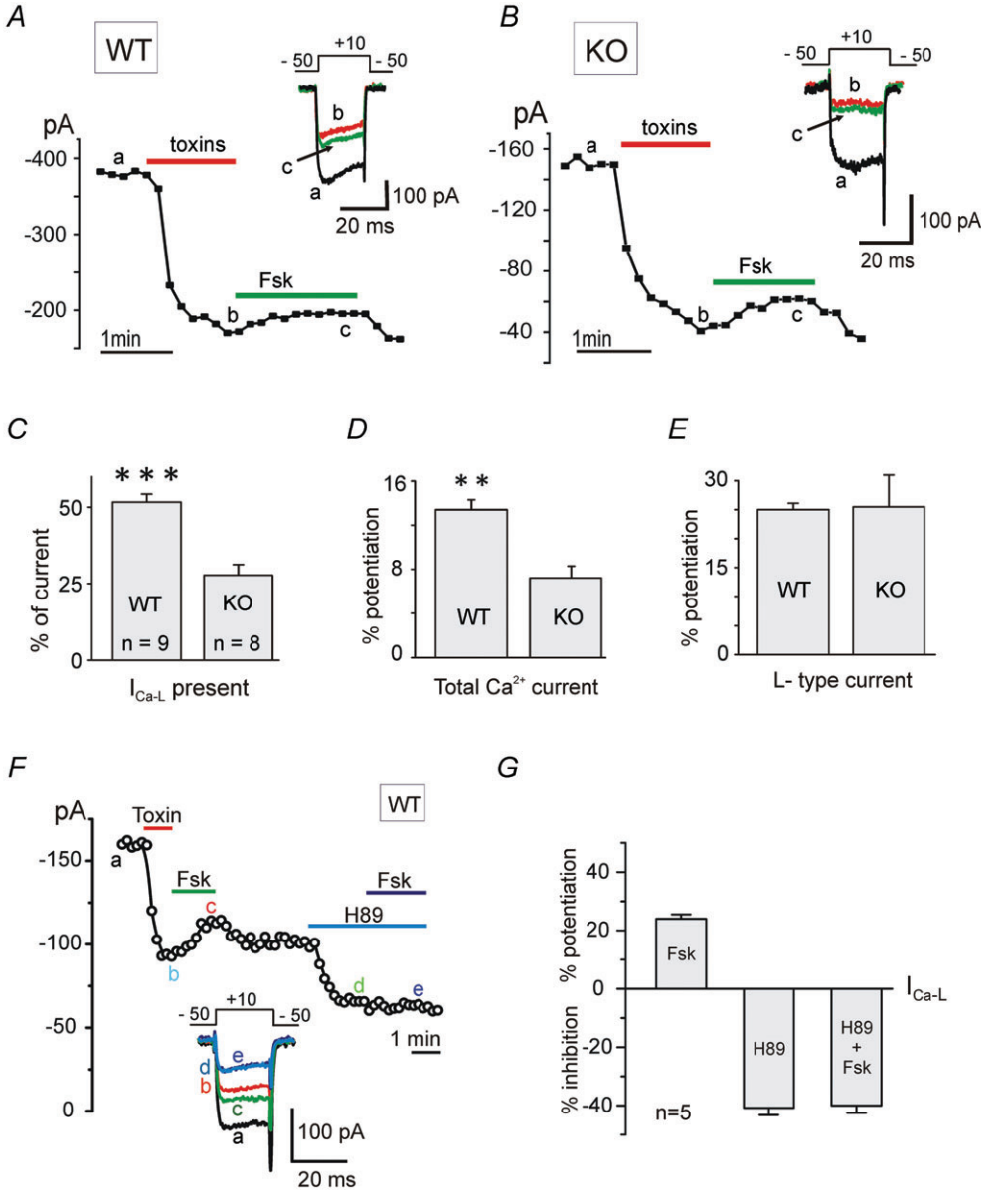

Figure 6. Forskolin potentiates the LTCCs remaining after blocking N-, P/Q- and R-type channels in WT and in Cav1.3$^{-/-}$ KO MCCs

A, Ca^{2+} current amplitude *vs.* time plot showing the reversible potentiation of L-type currents induced by forskolin (100 μM), after blocking N-, P/Q- and R-type HVA channels by a mixture of ω-Ctx-MVIIC (10 μM) + ω-Ctx-GVIA (3.2 μM) + SNX 482 (0.4 μM) in WT MCCs. SNX 482 was present in all solutions, including wash. Inset shows the current traces recorded at the time indicated by the letters. Same recording conditions as Fig. 5. Holding potential −50 mV. *B*, same experimental protocol as in *A* repeated in Cav1.3$^{-/-}$ (KO) MCCs. *C*, mean amplitudes of L-type currents remaining after blocking the non-L-type channels by the toxin mixture in WT ($n = 9$) and KO MCCs ($n = 8$) at V_h −50 mV (***$P < 0.001$, using unpaired Student's *t* test). *D*, mean I_{Ca} potentiation by forskolin in WT and KO MCCs (**$P = 0.006$). *E*, percentage of L-type currents potentiation by forskolin in WT (Cav1.2 + Cav1.3) and in KO MCCs (Cav1.2) normalized to the size of the currents reveal equal potentiation in WT and in KO MCCs ($P = 0.92$). *F*, the reversible potentiation of LTCC current by forskolin (100 μM) is prevented by the PKA blocker H89 (5 μM). Non-L-type currents were blocked by using the same toxin mixture used in *A*, except SNX 482. Same recording conditions as *A*. *G*, mean L-type current potentiation and inhibition induced by forskolin, H89 and H89 + forskolin. The current inhibition by H89 alone and in the presence of forskolin are not significantly different ($P = 0.82$; $n = 5$, Student's *t* test).

was very similar: 29.5 ± 3.1% before and 25.8 ± 3.8% after toxins application ($n = 5$; $P = 0.17$, not significantly different), proving that cGMP acts specifically on LTCCs in MCCs.

Cav1.2 and Cav1.3 channel currents are equally sensitive to cGMP

Given that LTCCs are selectively inhibited by cGMP, we next assessed how cGMP specifically affects Cav1.2 and Ca1.3 channel currents by comparing its action on the total I_{Ca} current in both WT and Cav1.3$^{-/-}$ KO MCCs. The representative time courses of control current and the effect of acute 8-pCPT-cGMP application on I_{Ca} in WT and KO MCCs are shown in Fig. 9*A* and *B*. As mentioned earlier, cGMP-mediated inhibition of LTCCs was slow and gradual and maximum inhibitory effects were attained within 2–3 min. Similarly, the washing followed a gradual recovery and was complete within the same amount of time. Quantitative inhibitions of I_{Ca} in WT and KO MCCs were 36.5 ± 2.2% ($n = 4$) and 19.2 ± 0.9% (**$P = 0.008$; $n = 6$; Fig. 9*C*), i.e. in a ratio of about 2:1 as expected if the inhibitory action of cGMP was equally affecting Cav1.2 and Cav1.3. Since Cav1.2 and Cav1.3 contribute equally to the total L-type Ca^{2+} current in MCCs (Fig. 4*C*), the 36% and 19% inhibition of I_{Ca} in WT and KO MCCs indicates that both Cav1.2 and Cav1.3 are equally sensitive to the cGMP-mediated inhibition.

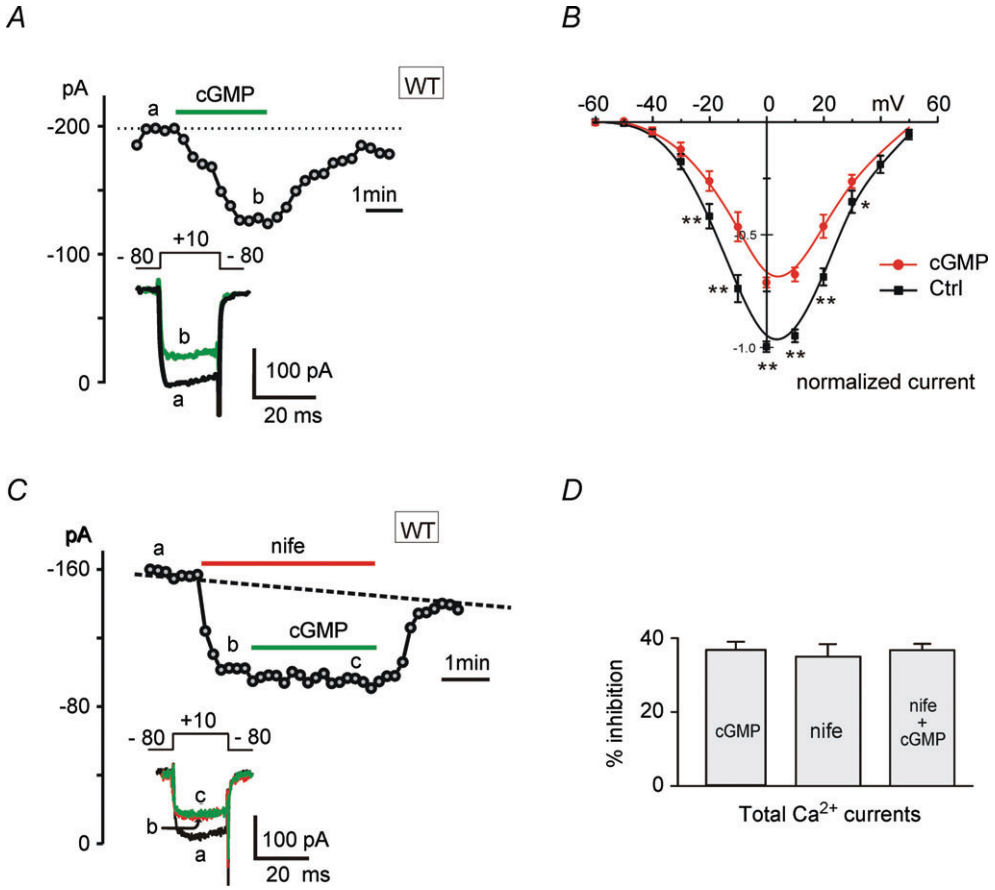

Figure 7. Nifedipine prevents the inhibition of I_{Ca} by 8-pCPT-cGMP in WT MCCs
A, Ca^{2+} current *vs.* time plot showing the reversible inhibition of I_{Ca} in WT MCCs by the cell-permeable cGMP analogue 8-pCPT-cGMP (1 mM). Inset shows the current traces recorded at the times indicated by the letters. Step depolarization to +10 mV was evoked from −80 mV (V_h) for 20 ms and repeated every 15 s. *B*, *I–V* relationships of total Ca^{2+} currents at control ($n = 14$) and during application of 1 mM 8-pCPT-cGMP ($n = 5$) obtained by 10 ms step depolarization to the indicated voltages for $n = 14$ (**$P < 0.01$, Student's *t* test). Holding potential −80 mV. *C*, plot of peak Ca^{2+} current recorded as a function of time in 2 mM extracellular Ca^{2+}. The inhibitory effect of PKG was prevented in the presence of nifedipine (3 μM) in 4 out of 7 cells. Inset shows the current traces recorded at the times indicated by the letters. Same protocols as in *A* except that step depolarizations were evoked every 10 s. *D*, mean percentage inhibition of I_{Ca} by 8-pCPT-cGMP, nifedipine and nifedipine + 8-pCPT-cGMP. The cGMP analogue in the presence of nifedipine produced no significant difference to the current block with nifedipine alone ($P = 1.0$).

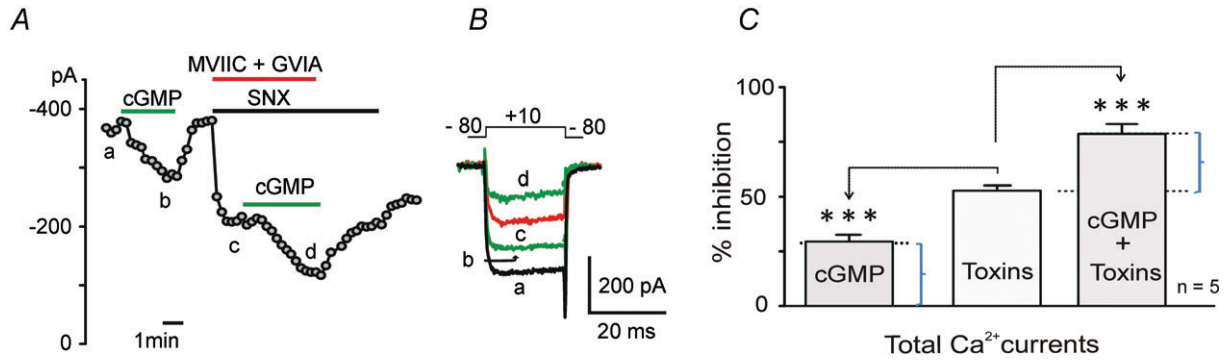

Figure 8. The cGMP-induced inhibition of I_{Ca} is preserved when Cav2 channels are blocked
A, plot of peak Ca^{2+} current recorded *vs.* time in 2 mM extracellular Ca^{2+} during application of 1 mM 8-pCPT-cGMP before and after Cav2 channels block by the toxin mixture. SNX 482 was present in all drug solutions, including first part of wash. In the second part of wash, SNX 482 was absent and recovery of R-type current was evident. Step depolarizations to +10 mV were evoked from −80 mV (V_h) for 20 ms and repeated every 20 s. *B*, current traces recorded at the times indicated by the letters in *A*. *C*, mean percentage inhibition of I_{Ca} obtained from $n = 5$ cells showing block of I_{Ca} by cGMP, toxin block of Cav2 channels (52.8 ± 2.3%) and block of cGMP in the presence of toxin. The toxin block of I_{Ca} *vs.* cGMP block alone and in the presence of toxin block is statistically different (***$P < 0.001$, one-way ANOVA followed by Bonferroni *post hoc* test). The cGMP effects before and after toxin treatment are not statistically different ($P = 0.17$, using Student's *t* test).

Cav1.2 and Cav1.3 are equally down-regulated by basal PKG activation

Similarly to PKA, which shows a prominent basal activity, we tested if also PKG is active under basal conditions by using 1 μM KT 5823, which is widely recognized to be a selective PKG blocker (Wahler & Dollinger, 1995; Murthy & Makhlouf, 1995; Abi-Gerges *et al.* 2001; Carabelli *et al.* 2002; Almanza *et al.* 2007), although some discrepancy exists (Burkhardt *et al.* 2000; Bain *et al.* 2003).

Since Cav1.2 and Cav1.3 channels are equally sensitive to cGMP-mediated inhibition, we assessed how both Cav1 isoforms are sensitive to PKG under basal conditions. We blocked PKG using KT 5823 (1 μM) and tested its potentiating action on LTCCs currents in WT (Cav1.2 + Cav1.3) and KO MCCs (Cav1.2). As illustrated in Fig. 10*A* and *B*, after stabilization of control currents, KT 5823 caused a slow but gradual potentiation of I_{Ca}. Maximal effects were achieved within 90–180 s, while washing was faster and complete within 60–90 s, indicating sustained basal levels of active PKG in MCCs. Quantitative potentiation by KT 5823 in WT and KO MCCs was 20.9 ± 1.2% ($n = 11$) and 9.7 ± 1.0% ($n = 7$; ***$P < 0.001$), respectively (Fig. 10*C*). Thus, as for PKA,

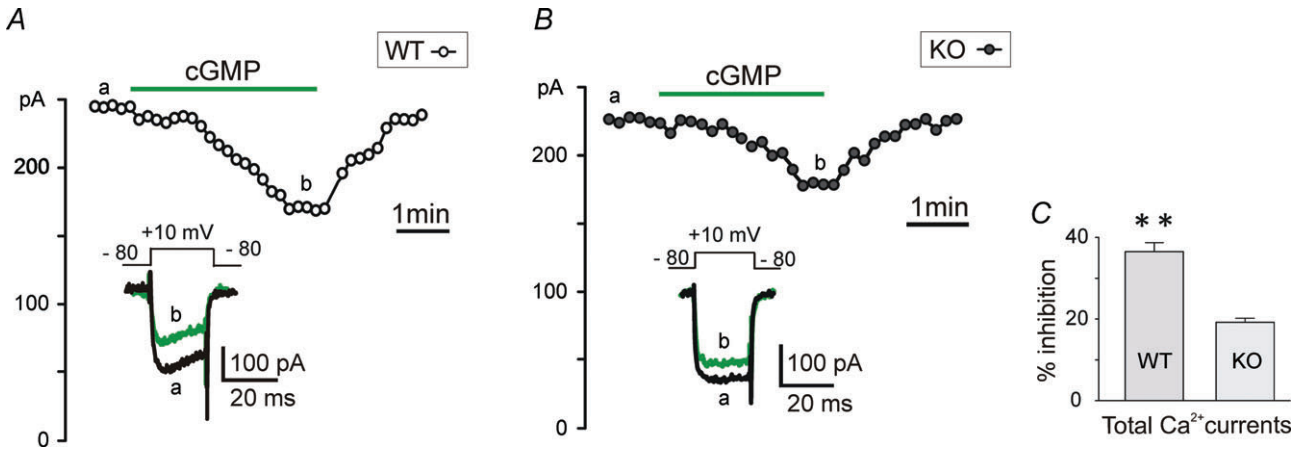

Figure 9. Comparative inhibition of I_{Ca} by pCPT-cGMP in WT and in Cav1.3$^{-/-}$ KO MCCs
A, Ca^{2+} current *vs.* time plot showing reversible inhibition of I_{Ca} in WT MCCs by 8-pCPT-cGMP (1 mM). Inset shows the current traces recorded at the times indicated by the letters. Current was evoked using a depolarizing pulse to +10 mV from −80 mV (V_h) for 20 ms and repeated every 10 s, in 2 mM extracellular Ca^{2+}. *B*, inhibition of I_{Ca} by 8-pCPT-cGMP in Cav1.3$^{-/-}$ (KO) MCCs. Same protocols as in *A*. *C*, the mean I_{Ca} inhibition induced by 8-pCPT-cGMP in WT ($n = 4$) and in KO MCCs ($n = 6$) are statistically significant (**$P = 0.008$, unpaired Student's *t* test).

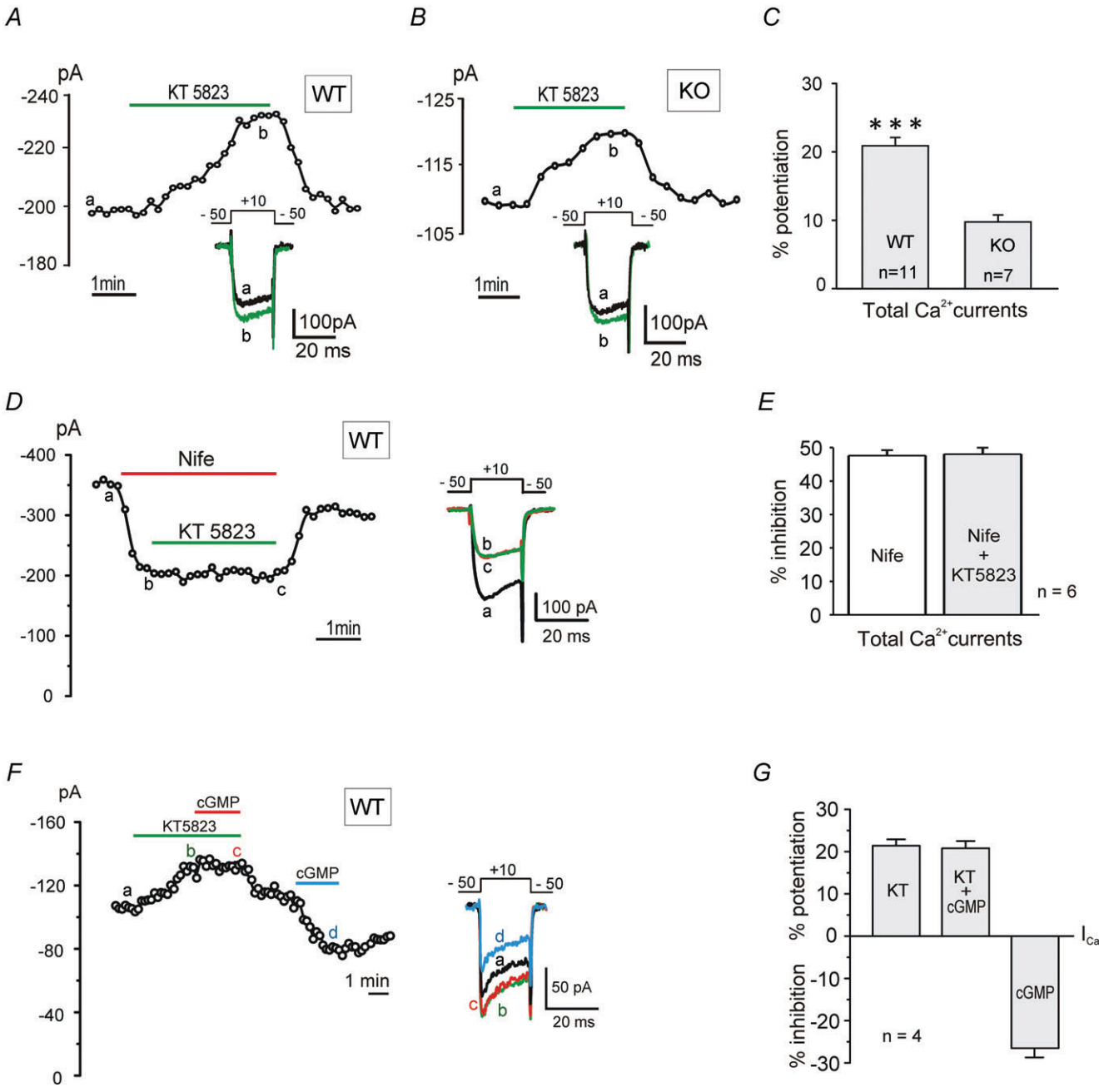

Figure 10. The PKG blocker KT 5823 potentiates I_{Ca} in WT and Cav1.3$^{-/-}$ KO MCCs and the action is prevented by nifedipine

A, Ca^{2+} current *vs.* time plot showing the reversible potentiation of basal I_{Ca} in WT MCCs by blocking PKG with KT 5823 (1 μM). Inset shows the current traces recorded at the times indicated by the letters. Current was evoked using a depolarizing pulse to +10 mV from −50 mV (V_h) for 20 ms in every 10 s in 2 mM extracellular Ca^{2+}. *B*, the reversible potentiation of I_{Ca} by KT 5823 in Cav1.3$^{-/-}$ KO MCCs (same protocols as in *A*) except that pulse was repeated every 20 s. *C*, mean basal I_{Ca} potentiation by KT 5823 in WT ($n = 11$) and in KO MCCs ($n = 7$), indicating significant differences (***$P < 0.001$, unpaired Student's *t* test). *D*, the selective PKG inhibitor KT 5823 does not produce any I_{Ca} potentiation in the presence of nifedipine. The inset shows the current traces recorded at the time indicated by the letters. *E*, mean I_{Ca} inhibitions with nifedipine alone and in presence of KT 5823 (1 μM) are nearly identical ($P = 0.63$, Student's *t* test), indicating that the potentiating effect of KT 5823 is prevented when LTCCs are blocked by nifedipine. *F*, KT 5823 (1 μM) prevents the inhibitory action of 8-pCPT-cGMP (0.1 μM). The action of the cGMP analogue is preserved when tested after washing out the PKG blocker. Same protocol conditions as in *A*. *G*, mean I_{Ca} potentiation by KT 5823 alone and in the presence of cGMP, and inhibition by cGMP alone. KT 5823-induced I_{Ca} potentiation is not affected by addition of 8-pCPT-cGMP in the presence of KT 5823 ($P = 0.78$; $n = 4$, Student's *t* test).

basal PKG inhibition in WT MCCs was twice as large as in KO MCCs and thus equally distributed on Cav1.2 and Cav1.3 channels.

To confirm that PKG inhibition by KT 5823 selectively potentiates LTCCs, we tested the effect of the PKG blocker on cells pre-treated with 3 μM nifedipine. The DHP completely prevented the potentiating effect of KT 5823 in WT MCCs (Fig. 10*D*), thus confirming that PKG-mediated phosphorylation selectively inhibits LTCCs at basal levels. Mean block by nifedipine was $47.6 \pm 1.6\%$ ($V_h = -50$ mV) and was nearly unaffected ($48.2 \pm 1.9\%$, $n = 6$; $P = 0.63$) by KT 5823 (Fig. 10*E*). In conclusion, in MCCs there exists a selective and prominent PKG-mediated basal inhibition of LTCCs which equally affects Cav1.2 and Cav1.3 channels. As a final control we tested whether KT 5823 was able to prevent the inhibitory effects of PKG in MCCs. Figure 10*F* and *G* shows the response of a representative cell, where exposure of 1 μM KT 5823 potentiates the I_{Ca} ($21.4 \pm 1.5\%$) and fully prevents the inhibitory action of PKG ($20.8 \pm 1.7\%$; $P = 0.78$) when elevated by 8-pCPT-cGMP (0.1 mM). Subsequent exposure to 8-pCPT-cGMP alone caused an average inhibition of $26.5 \pm 2.2\%$, ($n = 4$) that is not significantly different from that observed with 1 mM cGMP ($29.5 \pm 3.1\%$, $P = 0.78$; Fig. 8*C*).

PKA and PKG act synergistically and can induce extreme up- and down-modulation of Cav1 currents

The coexistence of opposing actions of PKG and PKA on Cav1.2 and Cav1.3 channels suggests that L-type currents can potentially undergo extreme variations if the two pathways act independently on LTCCs and are opposingly activated, i.e. if one pathway is activated and the other is inhibited at the same time. We tested this possibility by first activating PKA using forskolin and subsequently inhibiting PKG by applying KT 5823 to attain maximal up-regulation of L-type currents. Figure 11*A* shows that after blocking non-L-type currents with a toxin mixture containing MVIIC (10 μM), GVIA (3.2 μM) and SNX (400 nM) (trace b), exposure to forskolin alone caused a $32.4 \pm 0.7\%$ potentiation, while addition of KT 5823 increased the current by $45.3 \pm 0.9\%$ to give an overall synergistic potentiation of $77.7 \pm 0.5\%$ ($n = 4$, $^{***}P < 0.001$). The opposite was obtained when PKA inhibition by H89 was followed by PKG activation with 8-pCPT-cGMP (Fig. 11*B*). L-type currents persisting after blocking the non-LTCCs (trace b1) were down-regulated by $42.3 \pm 1.9\%$ with H89 and a further $44.1 \pm 4.5\%$ after addition of 8-pCPT-cGMP, to give an overall inhibition of $86.3 \pm 5.8\%$ in MCCs ($n = 4$, $^{***}P < 0.001$). We also found that by inverting the order of PKA and PKG modulators the results remained unchanged (data not shown), proving that both isoforms have distinct phosphorylation sites and that each phosphorylation pathway acts independently on Cav1.2 and Cav1.3 channels. In conclusion, the two opposing synergistic modulations of LTCCs are capable of generating L-type currents of one order of magnitude different amplitude: varying from a minimum of ~18% (PKG up, PKA down) to a maximum of ~180% (PKA up, PKG down) of control currents. This issue highlights the important role that PKA and PKG play in the modulation of LTCCs in MCCs.

Discussion

We provide evidence that the two LTCC isoforms expressed in MCCs, Cav1.2 and Cav1.3, are both effectively modulated by PKA and PKG under basal resting conditions and during maximal elevation of cAMP and cGMP levels. The two modulatory pathways act in opposition on LTCCs and markedly alter the size of L-type currents. Given that Cav1.2 and Cav1.3 regulate vital processes in chromaffin cells such as action potential firing, catecholamine secretion and vesicle endocytosis. These findings appear of key importance for understanding the molecular events that regulate chromaffin cell responses to opposing physiological conditions: stress-induced sympathetic stimuli *vs.* relaxed resting states where cAMP–PKA and cGMP–PKG levels could undergo extreme variations (Oset-Gasque *et al.* 1994; Wakade, 1998).

Of relevance is the observation that Cav1.3 is equally modulated as for Cav1.2, whose gating modifications by PKA and PKG have been extensively studied at the whole-cell and single channel level in cardiac cells (Bean *et al.* 1984; Hartzell & Fischmeister, 1986; Méry *et al.* 1993; Jiang *et al.* 2000). Little is known about the modulatory properties of native Cav1.3 channels (Catterall, 2011) and the present findings should partially overcome this missing information. Thanks to the availability of the Cav1.3$^{-/-}$ KO mice (Platzer *et al.* 2000) we could directly derive the modulation properties of Cav1.2 channels from the L-type currents of KO MCCs and those of Cav1.3 by comparing the different effects of PKA and PKG on the L-type currents of WT and Cav1.3$^{-/-}$ MCCs. Comparison was rather simple since Cav1.2 and Cav1.3 carry nearly the same quantity of Ca^{2+} current (Marcantoni *et al.* 2010; Mahapatra *et al.* 2011) and the single channel permeability properties of the two isoforms are remarkably similar (Jangsangthong *et al.* 2011; Bock *et al.* 2011).

We have also shown that cAMP–PKA and cGMP–PKG modulations act independently on Cav1 channels and their effects are cumulative. This is most evident when one pathway is activated and the other is inhibited. The two actions sum markedly, regardless of the sequential order in which activation and inhibition occur (S. Mahapatra, V. Carabelli & E. Carbone, unpublished observations)

and lead to extreme L-type current variations which can differ by one order of magnitude (from 18 to 180% of the control current) under extreme stimulation of one pathway and inhibition of the other. Comparable extreme effects are reported also for cardiac Ca^{2+} currents when separately enhanced by cAMP–PKA or down-regulated by cGMP–PKG (Hartzell & Fischmeister, 1986; Méry *et al.* 1993; Catterall, 2011). To our knowledge, the combined PKA- and PKG-mediated cumulative modulation of $I_{Ca\text{-}L}$ reported here represents one of the most impressive changes of L-type current amplitude driven by intracellular modulatory pathways, which is analogous to a 10-fold increase of Ca^{2+} channel density and represents a quick 'cell plasticity' change in a tissue where LTCCs regulate key cellular functions.

The cAMP–PKA-mediated up-regulation of Cav1.2 and Cav1.3 in MCCs

We have shown that like Cav1.2, Cav1.3 is also basally modulated by resting levels of PKA and can be effectively

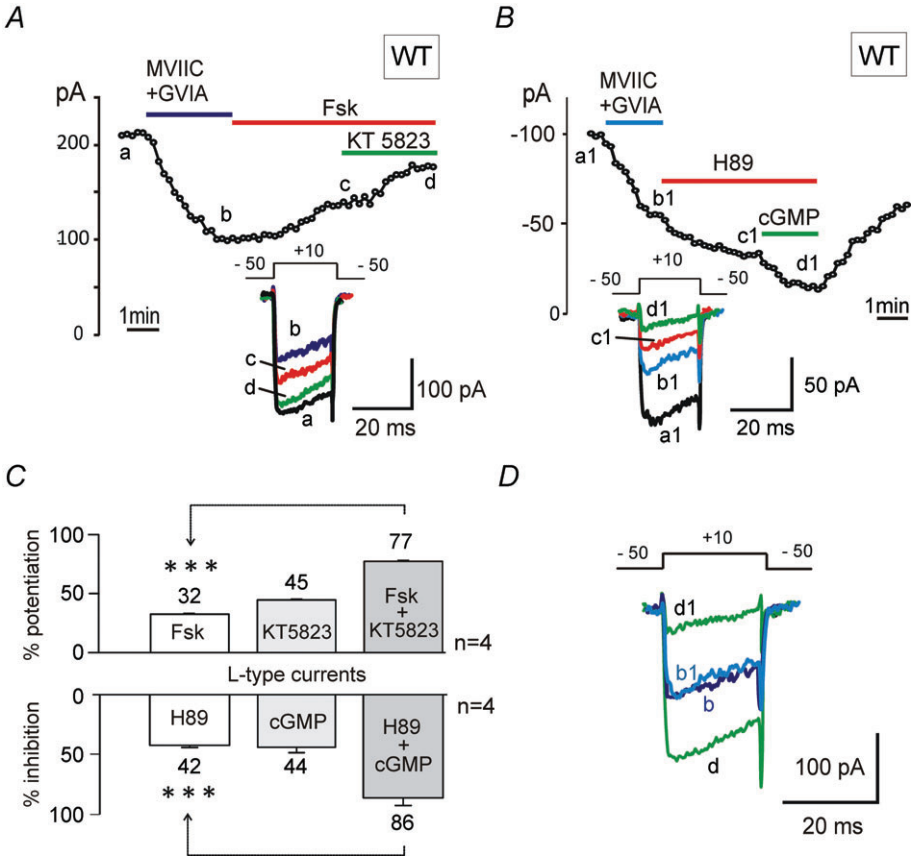

Figure 11. PKA activation and PKG inhibition cause the synergistic potentiation of LTCCs; in contrast, PKG activation and PKA inhibition cause opposite effects in WT MCCs
A, Ca^{2+} current *vs.* time plot showing the synergistic potentiation of $I_{Ca\text{-}L}$ in WT MCCs induced by the combined action of forskolin (100 μM) and KT 5823 (1 μM), after blocking the N- and P/Q-type channels with a mixture of ω-Ctx-MVIIC (10 μM) + ω-Ctx-GVIA (3.2 μM). The current was evoked using a depolarizing pulse to +10 mV from −50 mV (V_h) for 20 ms and repeated every 10 s, in 2 mM extracellular Ca^{2+}. *B*, plot of peak current recorded as a function of time showing the synergistic inhibition of $I_{Ca\text{-}L}$ current in WT MCCs induced by the combined action of H89 (5 μM) alone and together with 8-pCPT-cGMP (1 mM). Protocol conditions were similar to *A*. *C*, mean potentiation of $I_{Ca\text{-}L}$ in WT MCCs by forskolin alone and together with KT 5823 to give an overall synergistic potentiation of 77.7 ± 0.5% (***$P < 0.001$, Fsk *vs.* KT + Fsk, Student's *t* test) in 4 out of 17 cells (upper panel). In the lower panel are shown the mean $I_{Ca\text{-}L}$ inhibition by H89 alone and together with cGMP to give a final synergistic inhibition of 86.3 ± 5.8% (***$P < 0.001$, H89 *vs.* cGMP + H89, Student's *t* test), observed in 4 cells out of 4. *D*, overlapping of the synergistic potentiation and inhibition exhibited by Cav1 channel currents. Letters b and d denote basal Cav1 currents and maximal synergistic potentiation, when PKA is activated and PKG is inhibited. b1 and d1 denote basal Cav1 channel current and maximal synergistic inhibition, when PKA is inhibited and PKG is activated (data pulled out from panels *A* and *B*). The scale bar for current refers to the synergistic potentiation, and the synergistic inhibition was scaled up to facilitate visual comparison of up- and down-modulation of Cav1 channel currents by the two synergistic modulations.

up-regulated during sustained stimulations with forskolin. This represents a clear indication that native neuroendocrine Cav1.3 channels are up-regulated by PKA, in good agreement with works showing that: (i) recombinant Cav1.3 with potential serine PKA phosphorylation sites in the C-terminal tail are phosphorylated *in vitro* by incubation with the PKA catalytic subunit (Mitterdorfer *et al.* 1996), (ii) the C terminus of neuronal Cav1.3 co-localizes with the A-kinase anchoring protein 15 (AKAP15) to form a signalling complex with the β_2-adrenergic receptor (β_2-AR) in mouse brain (Marshall *et al.* 2011), (iii) the Ca^{2+} and Ba^{2+} currents carried by the long C-terminal splice variant of Cav1.3 (Cav1.3L) (Liang & Tavalin, 2007) and by the recombinant 180 kDa isoform of Cav1.3 (Qu *et al.* 2005) are effectively enhanced by intracellularly delivered PKA catalytic subunits and cAMP analogues. Thus, despite having distinct voltage ranges of activation and Ca^{2+}-dependent inactivation properties (Xu & Lipscombe, 2001; Koschak *et al.* 2001), Cav1.3 and Cav1.2 appear effectively up-regulated by cAMP–PKA both at basal levels and during sustained stimulation. This latter effect is interesting and could occur either during the autocrine β_1-AR stimulation driven by the adrenaline and noradrenaline released while MCCs are secreting (Cesetti *et al.* 2003), by selectively inhibiting phosphodiesterase type-4 (PDE4) (Marcantoni *et al.* 2009) or by the release of the pituitary adenylate cyclase-activating peptide (PACAP) during elevated sympathetic stimulation of the adrenal medulla (Przywara *et al.* 1996). In the first two cases, intracellular cAMP increases and the L-type currents of MCCs are effectively up-regulated (40% above the control level). As Cav1.3 has a direct role on pacemaking chromaffin cells (Marcantoni *et al.* 2010; Vandael *et al.* 2010), a cAMP–PKA-driven up-regulation of Cav1.3 could account for the increased amplitude of the nifedipine-sensitive sub-threshold Ca^{2+} current which drives the action potential up-stroke during spontaneous firing and is responsible for the increased firing frequency when blocking PDE4 (Marcantoni *et al.* 2009).

A cAMP–PKA-mediated up-regulation of Cav1.2 and Cav1.3 is expected to also exhibit a potentiating effect on the Ca^{2+}-dependent catecholamine secretion, which increases proportionally to the Ca^{2+} influx and the cAMP-mediated downstream processes controlling secretion (Carabelli *et al.* 2003). Since most of the secretion in chromaffin cells is uniformly controlled by all the Ca^{2+} channel types expressed in these cells (N, P/Q, R and L) (Engisch & Nowycky, 1996; Klingauf & Neher, 1997; Carabelli *et al.* 2003; Marcantoni *et al.* 2007), Cav1.2 and Cav1.3 are expected to contribute to vesicle fusion and catecholamine release proportionally to their increased current, without any specific preference for either one isoform. Obviously, since the two channels possess distinct voltage-dependent activation and inactivation kinetics (Koschak *et al.* 2001; Xu & Lipscombe, 2001), their PKA-mediated up-regulation is expected to reflect these features. Similar considerations are likely to hold true for the role that Cav1.2 and Cav1.3 play in controlling vesicle retrieval in chromaffin cells. Recent findings have shown that LTCCs control vesicle endocytosis (Rosa *et al.* 2007) and are functionally co-localized with clathrin and dynamin proteins (Rosa *et al.* 2010). Although there are not yet specific indications that either Cav1.2 or Cav1.3 regulate vesicle retrieval in MCCs, it would be of great interest to clarify this issue and test whether a cAMP–PKA induced up-regulation of both channels does indeed lead to an increased rate of endocytosis.

Concerning the modulatory effects of cAMP–PKA on Ca^{2+} currents, it is important to recall that, in contrast to LTCCs, the Cav2 channels (N, P/Q and R) are partially inhibited by forskolin and this action masks LTCCs potentiation induced by the adenylate cyclase (AC) activator (Figs 5 and 6). This occurs also in neostriatal dopaminergic neurones (Surmeier *et al.* 1995) and basal forebrain neurones (Momiyama & Fukazawa, 2007), where activation of dopamine D_1-receptors causes a PKA-mediated down-regulation of N- and P/Q-type channels which is prevented by PKA inhibitors. Similar to chromaffin cells, the up-regulation of LTCCs could be observed in a subset of neostriatal neurones only after blocking N- and P/Q-type channels (Surmeier *et al.* 1995). Regarding the possibilities that other protein kinases, besides PKA, could be involved in the up-regulation of Cav1 channels we should recall that the potentiating action of forskolin is fully prevented by H89 in MCCs (Fig. 6*F*) and that at the doses tested (1–5 μM) only few kinases (S6K1, MSK1, ROCK-II) could be inhibited by H89 (Davies *et al.* 2000). These kinases, however, are mainly involved in nuclear signalling pathways leading to cell growth and metabolism, inflammation and oxidative stress and other functions. Their modulatory effects develop slowly with time and there is no evidence supporting any specific action on Cav1 channels (Fenton & Gout, 2011; Mifsud *et al.* 2011; de-Godoy & Rattan, 2011).

The cGMP–PKG-mediated down-regulation of Cav1.2 and Cav1.3

We have clearly shown that L-type currents are effectively down-regulated by the cGMP–PKG signalling pathway, in good agreement with a number of reports on cardiac (Tohse & Sperelakis, 1991; Jiang *et al.* 2000; Yang *et al.* 2007), smooth muscles (Tewari & Simard, 1997; Ruiz-Velasco *et al.* 1998), neuronal (Kim *et al.* 2000; Nishiyama *et al.* 2003; Almanza *et al.* 2007; Lv *et al.* 2010) and chromaffin cells (Carabelli *et al.* 2002). Most of the studies report specific down-regulations of Cav1.2 that are probably mediated by two serine sites

located on the α1 subunit (Ser-1928 and Ser-533) (De Jongh *et al.* 1996; Jiang *et al.* 2000; Yang *et al.* 2007) while nothing is known about the down-regulation of recombinant Cav1.3 α1 isoform and the location of serine phosphorylation sites for PKG. The only available data on Cav1.3 modulation by cGMP–PKG comes from a study on the NO-mediated down-regulation of L-type currents in rat vestibular hair cells, which are mainly carried by Cav1.3 channels (Almanza *et al.* 2007). This work shows that part of the NO-induced inhibition of Cav1.3 is mediated by the cGMP–PKG pathway, thus proving an effective down-regulation of Cav1.3 channels by PKG (see also Lv *et al.* 2010). Our data are in very good agreement with these findings and show that the down-regulation of Cav1.3 is comparable with that of Cav1.2. The two isoforms are equally modulated at basal conditions and during stimulation with 8-pCPT-cGMP (Figs 9 and 10).

As previously noticed (Carabelli *et al.* 2002) our findings exclude also the possibility that the inhibitory effects of PKG on Cav1.2 and Cav1.3 channels derive from the activation of a cGMP-dependent cAMP-phosphodiesterase (PDE), which lowers the level of cAMP and reverses the cAMP-mediated up-regulation of LTCC activity. This action is typical of cardiac Cav1.2 channels (Méry *et al.* 1993; Wahler & Dollinger, 1995) and differs markedly from the one mediated by PKG described here. Indeed, we clearly showed that the inhibitory action of cGMP proceeds regardless of whether the cAMP–PKA pathway is fully blocked by H89 (Fig. 11*B*) or is maintained at sufficiently high levels under basal conditions in WT and Cav1.3$^{-/-}$ KO MCCs (Fig. 9). This occurs also during single channel recordings in bovine (Carabelli *et al.* 2002) and mouse chromaffin cells (S. Mahapatra, V. Carabelli & E. Carbone, unpublished observations) and proves that the two signalling pathways (cAMP–PKA and cGMP–PKG) affect mainly Cav1 channel gating without interfering with each other, most probably by phosphorylating distinct sites. In bovine chromaffin cells, PKG activation has identical inhibitory effects on L-type channel gating regardless of whether PKA is blocked by H89 or fully activated by 8-CPT-cAMP (Carabelli *et al.* 2002).

The synergistic effects of PKA and PKG on Cav1.2 and Ca1.3

An important issue of our work is that among the Ca^{2+} channel types expressed in MCCs, PKA and PKG mostly affect the LTCCs. PKG has no action on Cav2 channels (Fig. 7) while PKA has a partial inhibitory effect only during forskolin stimulation (Fig. 5). The two kinases, however, act independently on both Cav1.2 and Cav1.3 isoforms, and under extreme conditions of full up-regulation of one enzyme and down-regulation of the other, the effects become cumulative to give L-type Ca^{2+} currents of 10-fold different size. This is of great interest

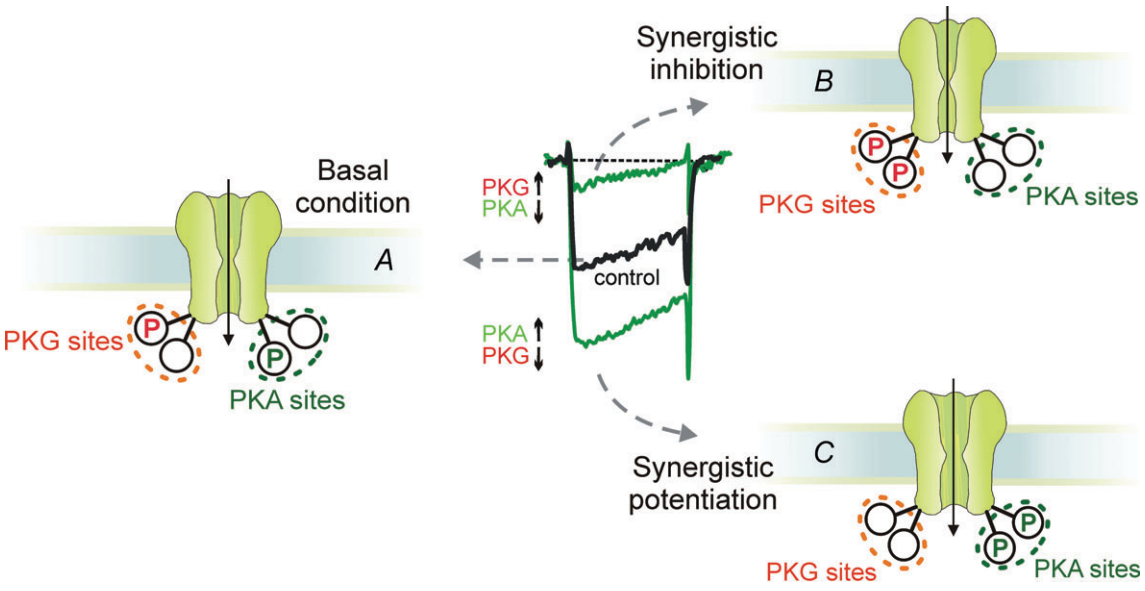

Figure 12. Schematic representation of Cav1 channel α1 subunit with two PKA and PKG phosphorylation sites (P), during basal conditions, synergistic potentiation and synergistic inhibition of LTCCs
Basally, both PKA and PKG P sites are partially phosphorylated and un-phosphorylated (*A*). Our synergistic experimental data suggest that phosphorylation and dephosphorylation driven by up- and down-regulation of PKA and PKG proceed independently of each other to reach two extreme conditions in which two PKA P sites are dephosphorylated and two PKG P sites are phosphorylated (*B*; minimal Cav1 current) or two PKA P sites are occupied and two PKG P-sites are dephosphorylated (*C*; maximal Cav1 current). The location of four P sites at the intracellular side is only indicative.

since these conditions may occur during chromaffin cell functioning and can be extrapolated to other cell tissues possessing the same signalling pathways (Ruiz-Velasco *et al.* 1998; Almanza *et al.* 2007). Figure 12 summarizes how these conditions could occur hypothetically by assuming two (or more) phosphorylation sites for PKG (red P) and an equal number of sites for PKA (green P). Under resting conditions (left panel) one of the two phosphorylation sites of PKG and PKA is occupied to give the basal L-type current (black trace). This setting justifies both the up-regulatory effects of PKG block by KT 5823 (following dephosphorylation of red P) and the opposing inhibitory effect of H89 during PKA block (following dephosphorylation of green P). Full phosphorylation of the two PKG sites and dephosphorylation of the PKA site lead to minimal L-type currents (top right panel), while full phosphorylation of the two PKA sites and dephosphorylation of the PKG site give maximal L-type current amplitude (bottom right panel). These two extreme conditions produce a nearly 10-fold change of L-type currents, which may influence action potential firing, catecholamine secretion and vesicle endocytosis if occurring during physiological states of MCCs and underline once more the great degree of modulation that Cav1 channels may undergo by the concomitant modulation of PKA and PKG pathways.

Functional implications of PKA and PKG modulation on Cav1 channels

As shown here and in previous works (Carabelli *et al.* 2001; Cesetti *et al.* 2003) the cAMP–PKA and cGMP–PKG pathways are already active at rest due to the basal activity of the two cyclases (AC and GC). AC is mainly activated by PACAP (Przywara *et al.* 1996), Ca^{2+} entry and αGs subunits that are activated by the basal activity of hormones and neurotransmitters released by sympathetic neurones (Anderson *et al.* 1992), surrounding capillaries (Wilson, 1988; Marley, 2003) and by the autocrine activity of chromaffin cells (Currie & Fox, 1996; Carabelli *et al.* 1998; Cesetti *et al.* 2003). This latter is most probably the cause of the high basal level of cAMP in culture conditions (2.2 mM) that rises 2- to 3-fold following β_1-adrenoreceptors (β_1-AR) stimulation and/or PDE selective inhibition (Marcantoni *et al.* 2009). The soluble GC is activated by the resting NO levels generated by the Ca^{2+}–calmodulin-mediated activation of NO synthase (NOS) expressed in most chromaffin cells (Oset-Gasque *et al.* 1994; Schwarz *et al.* 1998). Under these conditions, cGMP–PKG appears to work as a 'break' to limit the potentiating effects of cAMP–PKA and helps in setting the resting levels of Cav1.2 and Cav1.3 currents.

A potentiating synergistic effect of PKA and PKG could occur during sustained sympathetic stimulations that releases PACAP and induces massive secretion of adrenaline from chromaffin cells, which would further raise the levels of cAMP–PKA through the autocrine activation of the β_1-ARs expressed by RCCs and MCCs (Cesetti *et al.* 2003; Marcantoni *et al.* 2009). The increased Ca^{2+} entry during high-frequency stimulation could in turn activate the cGMP-specific Ca^{2+}–calmodulin-dependent PDE (PDE1) that regulates the resting levels of cGMP (Schwarz *et al.* 1998; Vicente *et al.* 2002). Thus, activation of a cGMP-specific PDE that lowers cGMP–PKG levels and the parallel increase of PKA during PACAP release and β_1-AR stimulation could markedly enhance Cav1.2 and Cav1.3 currents. This would sustain the rapid increase of firing activity and catecholamine release that ensure the fast activation of the 'fight-or-flight response' in chromaffin cells.

A reversed action (synergistic inhibition) could occur if chromaffin cells possess cGMP-activated PDE isoforms that hydrolyse cAMP (PDE2 and PDE3) (Lugnier, 2006). Any physiological up-regulation of the NO–cGMP–PKG pathway under these conditions would enhance cGMP and down-regulate cAMP which would rapidly depress Cav1.2 and Cav1.3 channel gating. The existence of other PDEs acting on cAMP beside PDE4, is supported by the findings that in MCCs the non-specific PDE blocker IBMX increases basal cAMP levels more potently than the PDE-4-specific blocker rolipram (Marcantoni *et al.* 2009).

Finally, it is worth noting that the present findings on Cav1.3 up- and down-regulation by PKA and PKG could have key physiological significance if extrapolated to the Cav1.3 channels of other tissues where the channel is highly expressed and functional. In cardiac sino-atrial and atrio-ventricular node cells, Cav1.3 contributes to the pacemaker current controlling heart beating (Mangoni *et al.* 2003; Zhang *et al.* 2011) and, thus, a β_1-AR or a NO–cGMP–PKG-driven modulation of its gating could either accelerate or decelerate the heart rate. Effective modulations driven by the cAMP–PKA and cGMP–PKG pathways could occur also to the Cav1.3 channels of cochlear inner hair cells (Marcotti *et al.* 2003) and dopaminergic neurons of substantia nigra pars compacta (Guzman *et al.* 2009) which control key functions of hearing sensory transduction and motor control.

References

Abi-Gerges N, Fischmeister R & Méry PF (2001). G protein-mediated inhibitory effect of a nitric oxide donor on the L-type Ca^{2+} current in rat ventricular myocytes. *J Physiol* **531**, 117–130.

Almanza A, Navarrete F, Vega R & Soto E (2007). Modulation of voltage-gated Ca^{2+} current in vestibular hair cells by nitric oxide. *J Neurophysiol* **7**, 1188–1195.

Anderson K, Robinson PJ & Marley PD (1992). Cholinoceptor regulation of cyclic AMP levels in bovine adrenal medullary cells. *Br J Pharmacol* **106**, 360–366.

Bain J, McLauchlan H, Elliot M & Cohen P (2003). The specificities of protein kinase inhibitors: an update. *Biochem J* **371**, 199–204.

Baldelli P, Hernández-Guijo JM, Carabelli V, Novara M, Cesetti T, Andrés-Mateos E, Montiel C & Carbone E (2004). Direct and remote modulation of L-channels in chromaffin cells: distinct actions on α1C and α1D subunits? *Mol Neurobiol* **29**, 73–96.

Bean BP, Nowycky MC & Tsien RW (1984). β-Adrenergic modulation of calcium channels in frog ventricular heart cells. *Nature* **307**, 371–375.

Bock G, Gebhart M, Scharinger A, Jangsangthong W, Busquet P, Poggiani C, Sartori S, Mangoni ME, Sinnegger-Brauns MJ, Herzig S, Striessnig J & Koschak A (2011). Functional properties of a newly identified C-terminal splice variant of Cav1.3 l-type Ca^{2+} channels. *J Biol Chem* **286**, 42736–42748.

Burkhardt M, Glazova M, Gambaryan S, Vollkommer T, Butt E, Bader B, Heermeir K, Lincoln TM, Walter U & Palmetshofer A (2000). KT 5823 inhibits cGPM-dependent protein kinase activity *in vitro* but not in intact human platelets and rat mesangial cells. *J Biol Chem* **275**, 33536–33541.

Carabelli V, Carra I & Carbone E (1998). Localized secretion of ATP and opioids revealed through single Ca^{2+} channel modulation in bovine chromaffin cells. *Neuron* **20**, 1255–1268.

Carabelli V, D'Ascenzo M, Carbone E & Grassi C (2002). Nitric oxide inhibits neuroendocrine Ca_V1 l-channel gating via cGMP-dependent protein kinase in cell-attached patches of bovine chromaffin cells. *J Physiol* **541**, 351–366.

Carabelli V, Giancippoli A, Baldelli P, Carbone E & Artalejo AR (2003). Distinct potentiation of L-type currents and secretion by cAMP in rat chromaffin cells. *Biophys J* **85**, 1326–1337.

Carabelli V, Hernández-Guijo JM, Baldelli P & Carbone E (2001). Direct autocrine inhibition and cAMP-dependent potentiation of single L-type Ca^{2+} channels in bovine chromaffin cells. *J Physiol* **532**, 73–90.

Catterall WA (2011). Voltage-gated calcium channels. *Cold Spring Harb Perspect Biol* **3**, a003947.

Cesetti T, Hernández-Guijo JM, Baldelli P, Carabelli V & Carbone E (2003). Opposite action of β1- and β2-adrenergic receptors on Cav1 L-channel current in rat adrenal chromaffin cells. *J Neurosci* **23**, 73–83.

Currie KPM & Fox AP (1996). ATP serves as a negative feed-back inhibitor of voltage-gated Ca^{2+} channel currents in cultured bovine chromaffin cells. *Neuron* **16**, 1027–1036.

Davies SP, Reddy H, Caivano M & Cohen P (2000). Specificity and mechanism of action of some commonly used protein kinase inhibitors. *Biochem J* **351**, 95–105.

De Godoy MA and Rattan S (2011). Role of rho kinase in the functional and dysfunctional tonic smooth muscles. *Trends Pharmacol Sci* **32**, 384–393.

De Jongh KS, Murphy BJ, Colvin AA, Hell JW, Takahashi M & Catterall WA (1996). Specific phosphorylation of a site in the full-length form of the α1 subunit of the cardiac L-type calcium channel by adenosine 3',5'-cyclic monophosphate-dependent protein kinase. *Biochemistry* **35**, 10392–10402.

Engisch KL & Nowycky MC (1996). Calcium dependence of large dense-cored vesicle exocytosis evoked by calcium influx in bovine adrenal chromaffin cells. *J Neurosci* **16**, 1359–1369.

Fenton TR & Gout IT (2011). Functions and regulation of the 70kDa ribosomal S6 kinases. *Int J Biochem Cell Biol* **43**, 47–59.

García AG, García-De-Diego AM, Gandía L, Borges R & García-Sancho J (2006). Calcium signalling and exocytosis in adrenal chromaffin cells. *Physiol Rev* **86**, 1093–1131.

García AG, Sala F, Reig JA, Viniegra S, Frías J, Fontériz R & Gandía L (1984). Dihydropyridine BAY-K-8644 activates chromaffin cell calcium channels. *Nature* **309**, 69–71.

García-Palomero E, Renart J, Andrés-Mateos E, Solís-Garrido LM, Matute C, Herrero CJ, García AG & Montiel C (2001). Differential expression of calcium channel subtypes in the bovine adrenal medulla. *Neuroendocrinology* **74**, 251–261.

Guzman JM, Sanchez-Padilla J, Chan CS & Surmeier DJ (2009). Robust pacemaking in substantia nigra dopaminergic neurons. *J Neurosci* **29**, 11011–11019.

Hartzell HC & Fischmeister R (1986). Opposite effects of cyclic GMP and cyclic AMP on Ca^{2+} current in single heart cells. *Nature* **323**, 273–275.

Hernández A, Segura-Chama P, Jiménez N, García AG, Hernández-Guijo JM & Hernández-Cruz A (2011). Modulation by endogenously released ATP and opioids of chromaffin cell calcium channels in mouse adrenalslices. *Am J Physiol Cell Physiol* **300**, C610–C623.

Hernández-Guijo JM, Carabelli V, Gandía L, García AG & Carbone E (1999). Voltage independent autocrine modulation of L-type channels mediated by ATP, opioids and catecholamines in rat chromaffin cells. *Eur J Neurosci* **11**, 3574–3584.

Jangsangthong W, Kuzmenkina E, Böhnke AK & Herzig S (2011). Single-channel monitoring of reversible L-type Ca^{2+} channel $Ca_V\alpha_1$-$Ca_V\beta$ subunit interaction. *Biophys J* **101**, 2661–2670.

Jiang LH, Gawler DJ, Hodson N, Milligan CJ, Pearson HA, Porter V & Wray D (2000). Regulation of cloned cardiac L-type calcium channels by cGMP-dependent protein kinase. *J Biol Chem* **275**, 6135–6143.

Kim SJ, Lim W & Kim J (1995). Contribution of L- and N-type calcium currents to exocytosis in rat adrenal medullary chromaffin cells. *Brain Res* **675**, 289–296.

Kim SJ, Song SK & Kim J (2000). Inhibitory effect of nitric oxide on voltage-dependent calcium currents in rat dorsal root ganglion cells. *Bioch Biophys Res Comm* **271**, 509–514.

Klingauf J & Neher E (1997). Modelling buffered Ca^{2+} diffusion near the membrane: implications for secretion in neuroendocrine cells. *Biophys J* **72**, 674–690.

Koschak A, Reimer D, Huber I, Grabner M, Glossmann H, Engel J & Striessnig J (2001). Alpha 1D (Cav1.3) subunits can form L-type Ca^{2+} channels activating at negative voltages. *J Biol Chem* **276**, 22100–22106.

Liang Y & Tavalin SJ (2007). Auxiliary β subunits differentially determine PKA utilization of distinct regulatory sites on Cav1.3 l-type Ca^{2+} channels. *Channels (Austin)* **1**, 102–112.

Lipscombe D, Helton TD & Xu W (2004). L-type calcium channels: the low down. *J Neurophysiol* **92**, 2633–2641.

Lopez MG, Albillos A, de la Fuente MT, Borges R, Gandia L, Carbone E, Garcia AG & Artalejo AR (1994), Localized L-type calcium channels control exocytosis in cat chromaffin cells. *Pflügers Arch* **427**, 348–354.

Lugnier C (2006). Cyclic nucleotide phosphodiesterase (PDE) superfamily: a new target for the development of specific therapeutic agents. *Pharmacol Ther* **109**, 366–398.

Lv, P, Rodriguez-Contreras A, Kim HJ, Zhu J, Wei D, Choong-Ryoul S, Eastwood E, Mu K, Levic S, Song H, Yevgeniy PY, Smith PJS & Yamoah EN (2010). Release and elementary mechanisms of nitric oxide in hair cells. *J Neurophysiol* **103**, 2494–2505.

Magnelli V, Pollo A, Sher E & Carbone E (1995). Block of non-L-, non-N-type Ca^{2+} channels in rat insulinoma RINm5F cells by ω-agatoxin and ω-conotoxin MVIIC. *Pflügers Arch* **429**, 762–771.

Mahapatra S, Calorio C, Vandael DHF, Marcantoni A, Carabelli V & Carbone E (2012). Calcium channel types contributing to chromaffin cell excitability, exocytosis and endocytosis. *Cell Calcium* **51**, 321–330.

Mahapatra S, Marcantoni A, Vandael DH, Striessnig J & Carbone E (2011). Are Cav 1.3 pacemaker channels in chromaffin cells? Possible bias from resting cell conditions and DHP blockers usage. *Channels (Austin)* **5**, 219–224.

Mangoni ME, Couette B, Bourinet E, Platzer J, Reimer D, Striessnig J & Nargeot J (2003). Functional role of L-type Cav1.3 Ca^{2+} channels in cardiac pacemaker activity. *Proc Natl Acad Sci U S A* **100**, 5543–5548.

Marcantoni A, Baldelli P, Hernandez-Guijo JM, Comunanza V, Carabelli V & Carbone E (2007). L-type calcium channels in adrenal chromaffin cells: role in pace-making and secretion. *Cell Calcium* **42**, 397–408.

Marcantoni A, Carabelli V, Vandael DH, Comunanza V & Carbone E (2009). PDE type-4 increases L-type Ca^{2+} currents, action potential firing and quantal size of exocytosis in mouse chromaffin cells. *Pflügers Arch* **457**, 1093–1110.

Marcantoni A, Vandael DH, Mahapatra S, Carabelli V, Sinnegger-Brauns MJ, Striessnig J & Carbone E (2010). Loss of Cav1.3 channels reveals the critical role of L-type and BK channel coupling in pacemaking mouse adrenal chromaffin cells. *J Neurosci* **30**, 491–504.

Marcotti W, Johnson SL, Rüsch A & Kros CJ (2003). Sodium and calcium currents shape action potentials in immature mouse inner hair cells. *J Physiol* **552**, 743–761.

Marley PD (2003). Mechanisms in histamine-mediated secretion from adrenal chromaffin cells. *Pharmacol Ther* **98**, 1–34.

Marshall MR, Clark III JP, Westenbroek R, Yu FH, Scheuer T & Catterall WA (2011). Functional roles of a C-terminal signaling complex of CaV1 channels and A-kinase anchoring protein 15 in brain neurons. *J Biol Chem* **286**, 12627–12639.

Méry PF, Pavoine C, Belhassen L, Pecker F & Fishmeister R (1993). Nitric oxide regulates cardiac Ca^{2+} current. Involvement of cGMP-inhibited and cGMP-stimulated phosphodiesterases through guanylyl cyclase activation. *J Biol Chem* **268**, 26286–26295.

Mifsud KR, Gutièrrez-Mecinas M, Trollope AF, Collins A, Saunderson EA & Reul JM (2011). Epigenetic mechanisms in stress and adaptation. *Brain Behav Immun* **25**, 1305–1315.

Mitterdorfer J, Froschmayr M, Grabner M, Moebius FF, Glossmann H & Striessnig J (1996). Identification of PK-A phosphorylation sites in the carboxyl terminus of L-type calcium channel a1 subunits. *Biochemistry* **35**, 9400–9406.

Momiyama T & Fukazawa Y (2007). D1-like dopamine receptors selectively block P/Q-type calcium channels to reduce glutamate release onto cholinergic basal forebrain neurones of immature rats. *J Physiol* **580**, 103–117.

Murthy KS & Makhlouf GM (1995). Interaction of cA-kinase and cG-kinase in mediating relaxation of dispersed smooth muscle cells. *Am J Physiol Cell Physiol* **268**, C171–C180.

Nagayama T, Matsumoto T, Kuwakubo F, Fukushima Y, Yoshida M, Suzuki-Kusaba M, Hisa H, Kimura T & Satoh S (1999). Role of calcium channels in catecholamine secretion in the rat adrenal gland. *J Physiol* **520**, 503–512.

Nishiyama M, Hoshino A, Tsai L, Henley JR, Goshima Y, Tessier-Lavigne M, Poo M-m & Hong K (2003). Cyclic AMP/GMP-dependent modulation of Cav1 channels sets the polarity of nerve growth-cone turning. *Nature* **423**, 990–995.

Oset-Gasque MJ, Parramón M, Hortelano S, Boscá L & González MP (1994). Nitric oxide implication in the control of neurosecretion by chromaffin cells. *J Neurochem* **63**, 1693–1700.

Peréz-Alvarez A, Hernández-Vivanco A, Caba-González JC, Albillos A (2011). Different roles of Cav1 channel subtypes in spontaneous action potential firing and fine tuning of exocytosis in mouse chromaffin cells. *J Neurochem* **116**, 105–121.

Platzer J, Engel J, Schrott-Fischer A, Stephan K, Bova S, Chen H, Zheng H & Striessnig J (2000). Congenital deafness and sinoatrial node dysfunction in mice lacking class D L-type Ca^{2+} channels. *Cell* **102**, 89–97.

Przywara DA, Guo X, Angelilli ML, Wakade TD & Wakade AR (1996). A non-cholinergic transmitter, pituitary adenylate cyclase activating polypeptide, utilizes a novel mechanism to evoke catecholamine secretion in ratadrenal chromaffin cells. *J Biol Chem* **271**, 10545–10550.

Qu Y, Baroudi G, Yue Y, El-Sherif N & Boutjdir M (2005). Localization and modulation of α1D (Cav1.3) L-type Ca channel by protein kinase A. *Am J Physiol Heart Circ Physiol* **288**, H2123–H2130.

Rodríguez-Pascual F, Miras-Portugal MT & Torres M (1996). Effect of cyclic GMP-increasing agents nitric oxide and C-type natriuretic peptide on bovine chromaffin cell function: inhibitory role mediated by cyclic GMP-dependent protein kinase. *Mol Pharmacol* **49**, 1058–1070.

Rosa JM, de Diego AM, Gandia L & Garcia AG (2007). L-type calcium channels are preferentially coupled to endocytosis in bovine chromaffin cells. *Biochem Biophys Res Commun* **357**, 834–839.

Rosa JM, Gandía L & García AG (2010). Permissive role of sphingosine on calcium-dependent endocytosis in chromaffin cells. *Pflügers Arch* **460**, 901–914.

Ruiz-Velasco V, Zhong J, Hume JR & Keef KD (1998). Modulation of Ca^{2+} channels by cyclic nucleotide cross activation of opposing protein kinases in rabbit portal vein. *Circ Res* **82**, 557–565.

Schwarz PM, Rodriguez-Pascual F, Koesling D, Torres M & Förstermann U (1998). Functional coupling of nitric oxide synthase and soluble guanylyl cyclase in controlling catecholamine secretion from bovine chromaffin cells. *Neuroscience* **82**, 255–265.

Sumii K & Sperelakis N (1995). cGMP-dependent protein kinase regulation of the L-type Ca^{2+} current in rat ventricular myocytes. *Circ Res* **77**, 803–812.

Surmeier DJ, Bargas J, Hemmings HC Jr, Nairn AC & Greengard P (1995). Modulation of calcium currents by a D1 dopaminergic protein kinase/phosphatase cascade in rat neostriatal neurons. *Neuron* **14**, 385–397.

Tewari K & Simard JM (1997). Sodium nitroprusside and cGMP decrease Ca^{2+} availability in basil arartery smooth muscle cells. *Pflügers Arch* **433**, 304–311.

Tohse N & Sperelakis N (1991). cGMP inhibits the activity of single calcium channels in embryonic chick heart cells. *Circ Res* **69**, 325–331.

Vandael DH, Gavello D, Zuccotti A, Knipper M, Marcantoni A & Carbone E (2011) SK channels slow down mouse chromaffin cells firing by accumulating subthreshold outward currents sensitive to block by intracellular Mg^{2+}. *2011 Abstract Viewer/Itinerary Planner*, Programme No. 234.02/C13. Society for Neuroscience, Washington, DC.

Vandael DH, Marcantoni A, Mahapatra S, Caro A, Ruth P, Zuccotti A, Knipper M & Carbone E (2010). Cav1.3 and BK channels for timing and regulating cell firing. *Mol Neurobiol* **41**, 185–198.

Vicente S, González MP & Oset-Gasque MJ (2002). Neuronal nitric oxide synthase modulates basal catecholamine secretion in bovine chromaffin cells. *J Neurosci Res* **69**, 327–340.

Wahler GM & Dollinger SJ (1995). Nitric oxide donor SIN-1 inhibits mammalian cardiac calcium current through cGMP dependent protein kinase. *Am J Physiol Cell Physiol* **426**, C45–C54.

Wakade AR (1998). Multiple transmitter control of catecholamine secretion in rat adrenal medulla. *Adv Pharmacol* **42**, 595–598.

Wilson SP (1988). Vasoactive intestinal peptide elevates cyclic AMP levels and potentiates secretion in bovine adrenal chromaffin cells. *Neuropeptides* **11**, 17–21.

Xu W & Lipscombe D (2001). Neuronal $Ca_V1.3$ $\alpha1$ L-type channels activate at relatively hyperpolarized membrane potentials and are incompletely inhibited by dihydropyridines. *J Neurosci* **21**, 5944–5951.

Yang L, Liu G, Zakharov SI, Bellinger AM, Mongillo M & Marx SO (2007). Protein kinase G phosphorylates Cav1.2 α1c and β2 subunits. *Circ Res* **101**, 465–474.

Zhang Q, Timofeyev V, Qiu H, Lu L, Li N, Singapuri A, Torado CL, Shin H-S & Chiamvimonvat N (2011). Expression and roles of Cav1.3 (α1D) L-type Ca^{2+} channel in atrioventricular node automaticity. *J Mol Cell Cardiol* **50**, 194–202.

Author's present address

A. Zuccotti: Department of Clinical Neurobiology, German Cancer Research Center (DKFZ), Heidelberg University Medical Center, 69120 Heidelberg, Germany.

Author contributions

S.M., A.M. and V.C. contributed to data collection and analysis of voltage-clamp experiments. A.Z. contributed to data collection and analysis of quantitative RT-PCR while working at the Department of Otolaryngology, University of Tubingen (Germany) under the supervision of Professor M. Knipper. S.M. and E.C. contributed to the conception and design of experiments, and the drafting of the article as well as revising it critically for important intellectual content. All authors have approved the final version of the manuscript. All experiments on Ca^{2+} current recordings were performed in the laboratories of the Department of Neuroscience at the University of Torino, Italy.

Acknowledgements

We thank Dr C. Franchino for preparing the cell cultures and Drs D. Vandael, D. Gavello and C. Calorio for helpful discussions. We also thank Professors Joerg Striessnig (Innsbruck) for helpful discussions and Jutta Engel (Homburg) for supplying the $Cav1.3^{-/-}$ KO mice. This work was supported by the Marie Curie Research Training Network 'CavNET' (Contract No. MRTN-CT-2006–035367), the Regione Piemonte POR/FERS program (grant no. 186-111C) and the UniTO-San Paolo Company research grant 2011–2013.